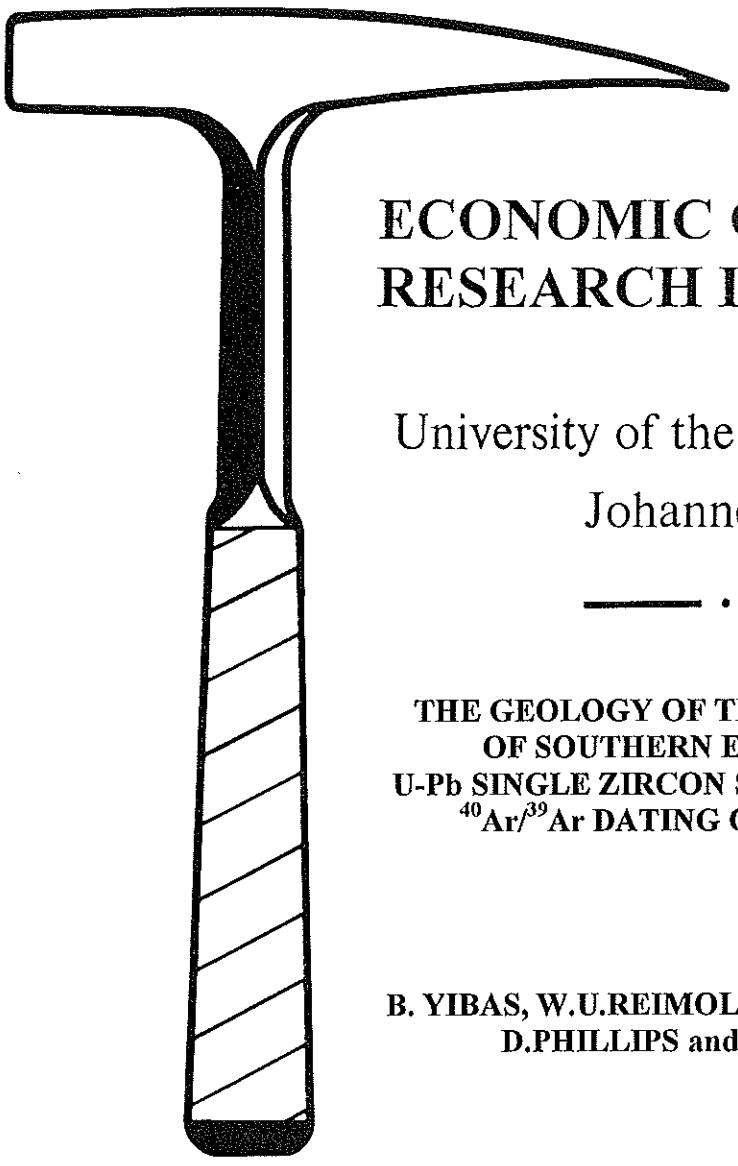

ECONOMIC GEOLOGY RESEARCH INSTITUTE

University of the Witwatersrand

Johannesburg

THE GEOLOGY OF THE PRECAMBRIAN OF SOUTHERN ETHIOPIA : II – U-Pb SINGLE ZIRCON SHRIMP AND LASER $^{40}Ar/^{39}Ar$ DATING OF GRANITOIDS

B. YIBAS, W.U.REIMOLD, R.A.ARMSTRONG, D.PHILLIPS and C. KOEBERL

INFORMATION CIRCULAR No.345

UNIVERSITY OF THE WITWATERSRAND
JOHANNESBURG

THE GEOLOGY OF THE PRECAMBRIAN OF SOUTHERN ETHIOPIA: II – U-Pb SINGLE ZIRCON SHRIMP AND LASER $^{40}Ar/^{39}Ar$ DATING OF GRANITOIDS

by

B. YIBAS[1], W. U. REIMOLD[1], R. A. ARMSTRONG[2], D. PHILLIPS[2] AND C. KOEBERL[3]

([1]Department of Geology, University of the Witwatersrand, Private Bag 3, WITS 2050, Johannesburg, South Africa; [2]Research School of Earth Sciences, The Australian National University, Canberra, ACT 0200, Australia; [3]Institute of Geochemistry, University of Vienna, Althan Str. 14, A-1090 Vienna, Austria)

ECONOMIC GEOLOGY RESEARCH INSTITUTE

INFORMATION CIRCULAR No. 345

July, 2000

THE GEOLOGY OF THE PRECAMBRIAN OF SOUTHERN ETHIOPIA: II- U-Pb SINGLE ZIRCON SHRIMP AND LASER $^{40}Ar/^{39}Ar$ DATING OF GRANITOIDS

ABSTRACT

The combined use of SHRIMP and laser probe $^{40}Ar/^{39}Ar$ dating, coupled with available field data, has led to the classification of the granitoids of the Precambrian of southern Ethiopia into seven generations. These, in descending order of age, include: Gt1 (>850 Ma); Gt2 (800-770 Ma); Gt3 (770-720 Ma); Gt4 (720-700 Ma); Gt5 (700-600 Ma); Gt6 (580-550 Ma); and Gt7 (550-500 Ma). The period 550 to 500 Ma (Gt7) is marked by emplacement of late- to post-tectonic and post-orogenic granitoids, such as the Metoarbasebat granite. Although the magmatic ages obtained from the SHRIMP zircon dating range from 880 to 526 Ma, the ^{40}Ar-^{39}Ar ages for all these samples are younger that 550 Ma. This suggests that the Gt7 period represents the latest tectonothermal event.

Five tectonothermal events belonging to the East African Orogen are recognised in the Precambrian of southern Ethiopia. These events include: (1) Adola (1157±2 to 1030±40 Ma); (2) Bulbul-Awata (~876±5 Ma); (3) Megado (800-750 Ma); (4) Moyale (700-550 Ma); and (5) Berguda (550-500 Ma). Two periods of charnockitic granitic magmatism and/or granulite facies metamorphism are recognised in the study area. The period between 710 and 730 Ma, which was dominated by the emplacement of charnockitic rocks (Yabello charnockitic granite-gneiss, Sagan basic charnockite, and Konso granulite), can be correlated with the widespread presence of charnockitic granites and granulite facies metamorphism from Sudan to Tanzania. The second phase of granulite facies metamorphism took place at the end of the Pan-African Orogeny and is represented by the charnockitic Berguda granitoid in the western part of the study area (~530 Ma). This age is similar to the ages of Pan-African granulites in other parts of the East African Orogen where granulite facies metamorphism and associated deformation occurred between 553 and 521 Ma - the postulated time of initial Gondwana amalgamation.

oOo

THE GEOLOGY OF THE PRECAMBRIAN OF SOUTHERN ETHIOPIA: II - U-Pb SINGLE ZIRCON SHRIMP AND LASER $^{40}Ar/^{39}Ar$ DATING OF GRANITOIDS

CONTENTS

oOo

Published by the Economic Geology Research Institute
Department of Geology
University of the Witwatersrand
1 Jan Smuts Avenue
Johannesburg 2001

ISBN 1-86838-289-3

THE GEOLOGY OF THE PRECAMBRIAN OF SOUTHERN ETHIOPIA: II -U-Pb SINGLE ZIRCON SHRIMP AND LASER $^{40}Ar/^{39}Ar$ DATING OF GRANITOIDS

INTRODUCTION

Although the Precambrian of southern Ethiopia occupies an important position within the East African Orogen (cf. fig.1 of Yibas et al., 2000), the available geochronological data for the Ethiopian Precambrian terranes, in general, and for southern Ethiopia, in particular, are still very limited (Table 1). In the 1990s, however, geochronological data have slowly emerged. Ayalew et al. (1990) carried out U-Pb zircon and Rb-Sr dating on 5 samples of plutonic rocks of the western Ethiopian Precambrian shield. In addition, some radiometric dating has been conducted on samples from syn- and post-tectonic granitoids of the northern Ethiopian Precambrian shield (Alemu, 1997; Tadesse et al., 1997; Tadesse et al., 2000).

Worku (1995) carried out U-Pb zircon, Rb-Sr and Sm-Nd dating on a few granitoid samples from the Adola Belt. Mechessa (1996) undertook limited ^{40}Ar-^{39}Ar dating with the aim of determining the age of the gold mineralisation of the Lega Dembi gold deposit and its relationship to adjacent granitoids. Teklay et al. (1993, 1998) also obtained a few age data on southern and eastern Ethiopian Precambrian granitoids (Table 1).

Although these geochronological data for the study area are, to some extent, useful in shedding light on the timing of magmatic activity, they still fall short of providing a comprehensive understanding of the evolution of the Precambrian terrane of southern Ethiopia. This has been primarily due to the lack of systematic geological and structural work in this region, which has severely constrained the use of geochronological data in interpreting the geological evolution of the study area. Recently, a new geological map for southern Ethiopia was completed, which now provides a basis for a new tectonostratigraphic classification of the Precambrian of southern Ethiopia (Yibas, 2000; Yibas et al., 2000).

This paper presents the SHRIMP and ^{40}Ar-^{39}Ar data for selected granitoids of the study area. These new results compliment the previously existing chronological data (Table 1), and together with the systematic geological mapping of the area (Yibas 2000; Yibas et al., 2000), make a significant contribution to deciphering the tectonic evolution of the Precambrian of southern Ethiopia and its significance within the East African Orogen.

Geological Outline

The Precambrian of southern Ethiopia occupies an important position between the Pan-African Mozambique Belt and the Arabo-Nubian Shield, which together form the East African Orogen (Stern, 1993, 1994) (fig.1 of Yibas et al., 2000). The relationship between the roughly contemporaneous high-grade metamorphic Mozambique Belt and the low-grade metamorphic Arabo-Nubian Shield in Northeast Africa is still subject of debate (e.g., Key et al., 1989).

In the Kenyan part of the East African Orogen, useful contributions to filling this gap of information have resulted from mapping in western (Vearncombe 1983) and north-central Kenya (Key et al., 1989). Whilst a number of geological investigations aimed at understanding the geology of selected areas in the Precambrian of southern Ethiopia (e.g., Lebling,1940; Jelenc, 1966, Gilboy, 1970; Chater, 1971; Kazmin,1972; Kazmin et al., 1978; Kozyrev et al., 1985; Gichile, 1991; Bonavia and Chorowicz, 1993; Woldehaimanot, 1995; Worku and Schandelmeier, 1996) have been conducted, a systematic geological investigation

Table 1. Available geochronological data for Precambrian rocks of southern Ethiopia

Lithotectonic Terrane	Complex	Locality	Rock type	Mi./WR.	Age	(*)
Gneiss - Granitoid Terrane	Moyale-Sololo Complex	El Der	Hornblende-biotite-gneiss	Bi (K-Ar)	749 ± 15	(1)
	Genale-Dolo Complex	Negele	Biotite-gneiss	Bi (K-Ar)	516 ± 5	(1)
		Zembaba village	Porphyritic granite (ET9)	Zr (Pb-Pb)	752 ± 6	(5)
		Zembaba village	Metarhyolite (ET10)	Zr (Pb-Pb)	605 ± 7	(5)
		Alge[1], west of the Bulbul Belt	MyloniticTonalite (Alge Gneiss of Kazmin, 1972)	Zr (Pb-Pb)	557± 9	(5)
		35 km SW Negelle (Bulbul)	Porphyritic Granodiorite Gneiss	Zr (Pb-Pb)	884 ± 7	(5)
	Adola Complex	Mormora River	Granite	Bi (K-Ar)	504 ± 20	(2)
		Burjiji	Granite	Zr (U-Pb)	612 ± 6	(7)
		Gariboro	Pegmatite Granite Granite Granite	Ms (Rb-Sr) WR (Rb-Sr) WR (Rb-Sr) Zr (U-Pb)	530 ± 10 680 515 ± 10 646 ± 30	(3) (3) (3) (7)
		Lega Dima	Granite	Zr (U-Pb)	550 ± 18	(7)
		Robele	Granite	Zr (U-Pb)	554 ± 13	(6)
		Alghe[1] (west of Digati)	Alghe granite-gneiss	Zr (U-Pb)	722 ± 2	(7)
		Sebeto	Tonalite gneiss	Zr (U-Pb)	765 ± 3	(6)
	Burji-Finchaa Complex	Yabello town	Yabello granite-gneiss	Zr (Pb-Pb)	716 ± 8	(5)
		Agere Mariam	Foliated granite	Zr (U-Pb)	708 ± 3	(6)
		Near Agere Mariam	Berguda granite	Zr (U-Pb)	529± 11	(6)
		Konso, west of Burji-Finchaa Complex	Konso Granulite	Zr (Pb-Pb)	720± 7	(5)
Ophiolitic Fold and Thrust Belts	Megado Belt	Megado	Megado metabasic rocks	Sm-Nd (WR)	789 ± 36	(7)
	Moyale-El Kur Belt	Moyale	Quartz diorite	Bi (K-Ar)	526 ± 5	(1)
		Moyale	Meta-trondhjemite	Zr (Pb-Pb)	658 ± 8	(5)
		El Der	Amphibolite	WR (K-Ar)	647 ± 20	(1)
		Moyale	Amphibolite	Zr (U-Pb)	700 ± 10	(5)

(*) Source: (1) Rogers et al. (1965); (2) Jelenc (1966); (3) Gilboy (1970); (4) Ethiopian Institute of Geological Surveys, unpublished data; (5) Teklay et al. (1993); (6) Abraham et al. (1992); (7) Worku (1996). WR = whole rock, Mi = mineral, Bi = biotite, Zr = zircon, Ms = muscovite.

[1]Note that Alghe and Alge are two different localities, the former located in the western margin of the Megado Belt near Digati village, and the latter in the westernmost part of the Genale-Dolo complex, west of the Bulbul Belt.

covering the entire tract of the Precambrian of southern Ethiopia has only recently been attempted (Yibas 2000; Yibas et al., 2000).

The Precambrian terrane of southern Ethiopia is bounded to the west by the Main Ethiopian Rift System (MERS) and its associated volcanics, and to the east by Mesozoic sediments. The

Precambrian rocks comprise high-grade ortho- and para-gneisses and migmatites, low-grade volcano-sedimentary-ultramafic assemblages, and granitoids of variable composition (Fig. 1). Kazmin (1972) and Kazmin et al. (1978) classified the Precambrian rocks of Ethiopia into Upper, Middle and Lower Complexes, following the three-fold classification of Gilboy (1970) and Chater (1971) for rocks of the Adola area. According to this classification, the Lower Complex of relatively high-grade gneisses represents the older (presumably Archaean)

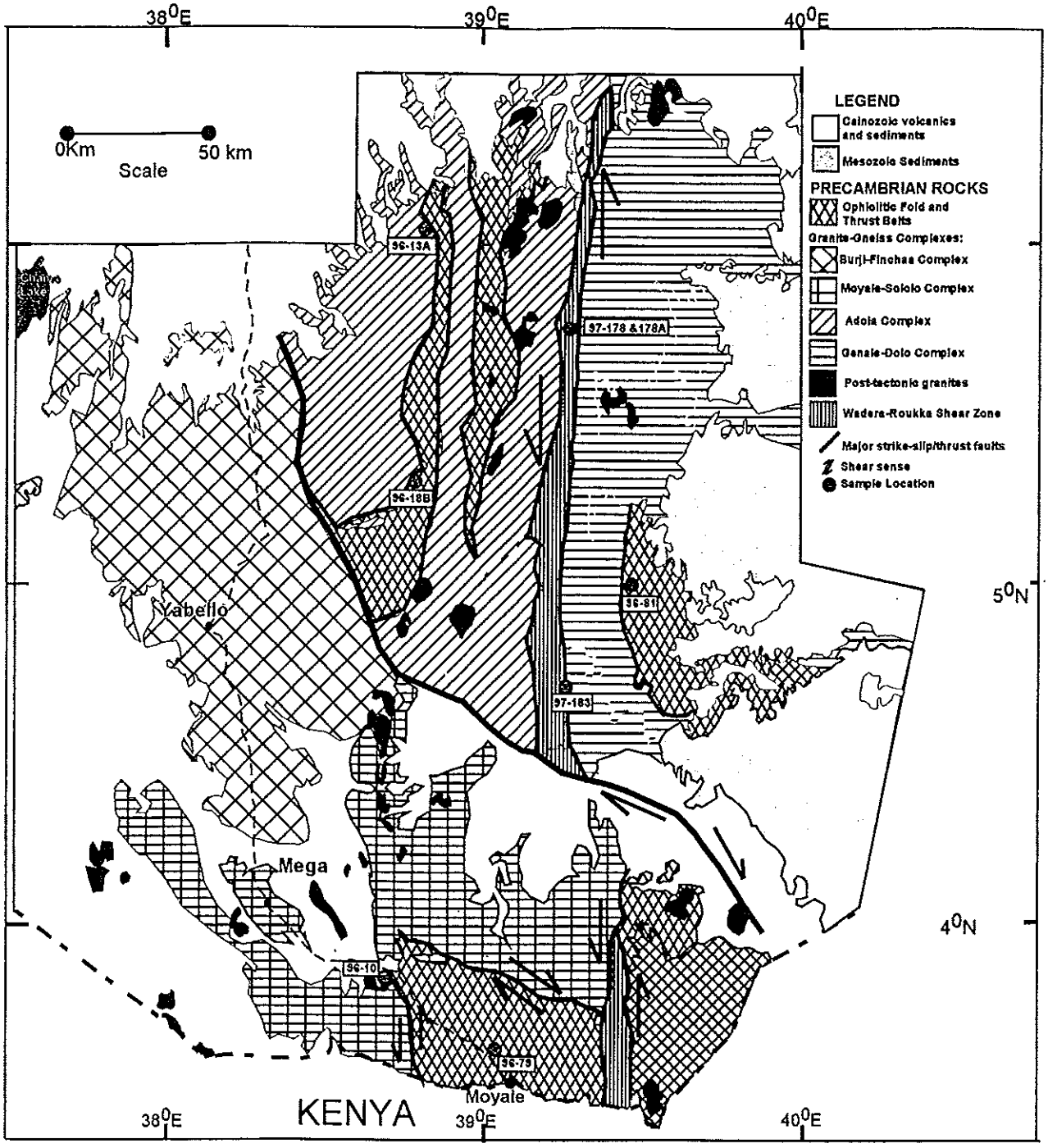

Figure 1: Simplified geological map of southern Ethiopia with sample location of dated rocks (modified from Yibas, 2000).

cratonic basement, upon which the Middle Complex (Lower to Middle Proterozoic, platform cover clastic sediments) was deposited. The Upper (Upper Proterozoic) Complex consists of low-grade volcanosedimentary assemblages of ophiolitic affinity (Kazmin et al., 1978).

Recently, a comprehensive geological map of an ~88000 km^2 area in southern Ethiopia, together with a new tectonostratigraphic classification for the Precambrian of southern Ethiopia, has been prepared (Yibas et al., 2000). According to these workers, the Precambrian of southern Ethiopia comprises two distinct tectonostratigraphic assemblages (terranes), separated by repeatedly reactivated structural zones. These assemblages are referred to as: (1) the Granite-Gneiss Terrane, which in turn is classified into complexes; and (2) ophiolite fold and thrust belts (Yibas et al., 2000; Fig. 1).

The bulk of the Granite-Gneiss Terrane is formed by para- and ortho-quartzofeldspathic gneisses, intercalated with amphibolites, sillimanite-kyanite-bearing schist and marbles, and granitoids, and extends into northern Kenya. Lithologically, the paragneisses are correlative with the gneisses of northern Kenya (Yibas 2000; Yibas et al, 2000).

GRANITOIDS

Several generations of felsic to intermediate intrusives occur in the Precambrian of southern Ethiopia (cf. Yibas et al., 2000). These granitoids range from gneisses and migmatites to undeformed granites and vary compositionally from diorites to granites, with the dioritic rocks being less abundant (Yibas, 2000). The gneissose granitoids form an integral part of the Granite-Gneiss Terrane, but are absent or rare in the ophiolitic fold and thrust belts. Based on field relationships, structures, petrographic descriptions, textures, and contact relationships with adjacent lithologies, the granitoids of southern Ethiopia can be broadly classified into granitoid gneisses, deformed granitoids and undeformed (post-tectonic) granitoids.

Granitoid Gneisses

The major granitoid gneisses in southern Ethiopia include the Bulbul mylonitic diorite gneiss, Melka Guba megacrystic diorite gneiss, Sebeto tonalite gneiss, Alghe granite-gneiss, Wadera megacrystic diorite gneiss and Yabello charnockitic granite-gneiss (cf. fig. 3 of Yibas et al., 2000). In most cases these granitoids have undergone intense metamorphism and deformation.

Deformed Granitoids

Conspicuous examples of this granite phase include the Gariboro and Burjiji massifs, the Moyale granodiorite and the Meleka granodiorite. These rocks are often foliated, in places gneissose, and form elongated bodies parallel to the regional foliation trends. Most of these granites were considered of syntectonic origin (Kazmin 1972, 1975; Tefera et al., 1990).

Late- to Post-tectonic Granitoids

Most of the granites, which represent the final phase of granitic magmatism in southern Ethiopia, occur in the high-grade gneisses. Their contact relationships with the country rocks, where exposed, are sharp, steep and discordant to the regional foliation. The size of these granitic bodies is variable, but when compared to the other suites of granites, they generally are smaller.

Four samples from the granitoid gneisses [viz., the Bulbul mylonitic diorite gneiss (BY 96-78); the Melka Guba megacrystic diorite gneiss (BY97-183); the Digati diorite gneiss (BY96-18); and the Wadera megacrystic diorite gneiss (BY97-178)], three samples from the deformed granitoids [the Moyale granodiorite (BY 97-79); the Meleka metagranodiorite (BY96-13A); and the Wadera foliated granite dyke (BY97-178A)], and one from an undeformed granitoid [the Metoarbasebat granite (BY 96-13A), (Fig. 1)] were dated using SHRIMP and Ar-Ar laser probe dating techniques. These samples were selected on the basis of relative deformation intensities and crosscutting relationships so as to analyse the different magmatic events that occurred in the Precambrian of southern Ethiopia.

METHODOLOGY

Ion Microprobe (SHRIMP) U-Pb Zircon Dating

Despite the advances made in geochronological techniques, deciphering the geochronology of complex metamorphic terranes is still challenging as problems arise from overprinting of pre-existing assemblages by successive metamorphic event(s) and partial or complete resetting of geochronometers, such as K-Ar, ^{40}Ar-^{39}Ar and Rb-Sr, by younger tectonothermal events. The potential of within-grain analysis for determining the crystallisation history of zircons has been appreciated since the early 1970s. This followed the discovery, from conventional dating techniques, that old zircon grains had preserved their ages through Alpine-age granulite-facies metamorphism, and that xenocrysts in some granites had survived fusion temperatures (Compston et al., 1992).

The present study has been aimed at establishing a geochronological framework for the complex Precambrian terrane of southern Ethiopia, using the SHRIMP dating technique to determine precise U-Pb ages on single zircons from selected lithologies. In total, 8 samples were analysed. The zircons from one sample (granitic pegmatite sample BY97-180B, not discussed in this paper) were found to be extremely metamict (radiation-induced damage to the crystal lattice) because of their high concentrations of U and Th. This is not an unusual phenomenon for zircons from rocks of this nature, but precluded any meaningful geochronological work being done on these particular zircons.

Zircons from the selected samples were separated using a Wilfley table, a magnetic separator, and heavy liquids at the Hugh Allsopp Laboratory, University of the Witwatersrand, Johannesburg. Zircon separates were submitted to the Precise Radiogenic Isotopic Services (PRISE), at the Research School of Earth Sciences (RSES), Australian National University (ANU) in Canberra. Zircon grains were handpicked under a binocular microscope and mounted in epoxy, together with the RSES SHRIMP zircon standards AS3 (Duluth Complex gabbroic anorthosite; Paces and Miller, 1989) and SL13.

The grains were then sectioned, polished and photographed. All zircons were further examined by SEM cathodoluminescence imaging, a procedure that greatly enhances the quality of data produced in the subsequent ion microprobe sessions. Through cathodoluminescence imaging of the zircons, hidden and complex internal structures can be more accurately determined than in normal reflected or transmitted light, and consequently, the target area can be more reliably selected for analysis. Using this approach, it was also possible to get more information on inheritance, metamorphic overgrowths and protolith ages.

The samples were analysed at the RSES using both the SHRIMP I and SHRIMP II instruments. The SHRIMP data have been reduced in a manner similar to that described by

Compston et al. (1992) and Williams and Claesson (1987). U/Pb isotopic ratios in the unknown samples were normalised to a $^{206}Pb/^{238}U$ value of 0.1859 (equivalent to an age of 1099.1 Ma) for AS3. The U and Th concentrations were determined relative to those measured in the SL13 standard. In most cases, ages were calculated using the $^{206}Pb/^{238}U$ ratios, with the correction for common Pb being made using the measured $^{207}Pb/^{206}Pb$ and $^{206}Pb/^{238}U$ values following Tera and Wasserburg (1972) and as described in Compston et al. (1992). In those cases where it was more appropriate to use the radiogenic $^{207}Pb/^{206}Pb$ compositions to calculate ages, the ages were determined using the directly measured $^{204}Pb/^{206}Pb$ ratios and the relevant model common Pb composition after Cumming and Richards (1975).

Uncertainties in the isotopic ratios and ages in the data tables (and in the error bars in the plotted data) are reported at the 1σ level, but final weighted mean ages are reported with 95% confidence limits (2σ).

$^{40}Ar/^{39}Ar$ Dating

^{40}Ar-^{39}Ar data from biotite, amphibole, and muscovite were obtained at the Anglo American Research Laboratories (AARL), Johannesburg. Samples were crushed and sieved. Some twenty biotite/muscovite/amphibole grains were extracted for analysis. The grains were ultrasonically cleaned in de-ionised water and acetone and visually inspected for signs of alteration. The grains were then packed into the centre of aluminium foil pockets and placed into an evacuated quartz glass vial, together with the irradiation standard Hb3gr (Turner, 1971). Flux monitors were placed within 2mm of the sample packet. Neutron irradiation was carried out in position B2W of the Safari-1 reactor, Pelindaba (South Africa), for a period of 40 hours at 10MW.

After irradiation and cooling, grains were individually loaded into 1 mm-diameter wells in a 22 mm-diameter aluminium disk. The disk was then covered with a sapphire glass cover slip to ensure containment and to protect the coated quartz glass window of the high vacuum sample port. Prior to analysis the samples were baked at ~200°C for 12 hours to remove adsorbed volatiles. Fifty individual Hb3gr grains from five irradiation positions were analysed in order to calculate an average J-value.

Core/rim analyses were carried out using single pulses from a focused infrared laser beam. Gas purification was achieved by means of two AP10 getter pumps, operated at 400°C and 20°C, respectively. Argon analyses were carried out on a MAP 215-50 static mass spectrometer, equipped with a Nier-type source and Johnson multiplier detector, and operated at a mass resolution of ~600. Procedural blanks were 7×10^{-17} moles for ^{40}Ar, 2×10^{-16} moles for ^{39}Ar and ^{38}Ar, 5×10^{-17} moles for ^{37}Ar, and 4×10^{-18} moles for ^{36}Ar. Mass discrimination was monitored by analyses of standard air volumes from a Doerflinger pipette system. Analyses of co-irradiated calcium and potassium salts yielded the following isotope production ratios: $(^{39}Ar/^{37}Ar)_{Ca} = 0.000754 \pm 0.000027$; $(^{36}Ar/^{37}Ar)_{Ca} = 0.000319 \pm 0.000010$; $(^{40}Ar/^{39}Ar)_K = 0.031 \pm 0.005$. These values compare favourably with analyses of a previous batch of salts, which were analysed by R. Burgess at Manchester University. The latter analysis yielded ratios of 0.000708 ± 0.000024; 0.000312 ± 0.00002; and 0.036 ± 0.008, respectively.

All reported data have been corrected for the system blanks, mass discrimination, radioactive decay of ^{39}Ar and ^{37}Ar, reactor interference, fluence gradients and atmospheric contamination.

Unless otherwise stated, errors are one sigma (1σ) uncertainties and include errors in the J-value estimates.

RESULTS

Metoarbasebat Granite

This granite occurs in the northern part of the Moyale-Sololo Granite-Gneiss Complex close to the Moyale ophiolitic fold and thrust belt (Fig.1, see also fig. 3 of Yibas et al., 2000) around Metoarbasebat village on both sides of the main Addis Ababa-Moyale road. It occurs as circular to semi-elliptical domes forming high topography. The granite is coarse-grained, pink to grey, and composed of K-feldspar, plagioclase, hornblende, and quartz. A NE-SW to ENE-WSW trending fabric, defined by mineral (mainly plagioclase, hornblende, and quartz grains) alignment, is discernible. The granite shows porphyritic texture with large phenocrysts of amphiboles and plagioclase. Coarse-grained quartz veins cut across the granite. Mafic xenoliths with diameters of 10 to 20 cm have been observed. As this granite is spatially close to the Moyale ophiolitic fold and thrust sub-belt (Fig. 1, 96-10), it is assumed that these xenoliths are derived from this sub-belt.

The zircons from sample BY96-10B of this granite are small (80-120 μm in length), colourless to light pink, and are mainly subhedral, with occasional acicular forms. Cathodoluminescence imaging revealed strong compositional zoning in most of the zircons, which also shows that some grains have cores of inherited zircon. These cores are surrounded by zoned overgrowths (Fig. 2a).

The U-Th-Pb results of the SHRIMP analyses for this granite are reported in Table 2 and are plotted on a Tera-Wasserburg U-Pb concordia diagram in Figure 3a. In this diagram, the data are plotted uncorrected for common Pb, with the measured analyses plotting on a mixing line between a radiogenic end-member (on concordia) and a common Pb composition. The lower the common Pb content of the zircon, the closer the data points plot to the concordia. As can be seen from Figure 3a, the majority of the data plot as a cluster near the concordia and, thus, have very low common Pb contents. One analysis (6.1, Table 2) plots away from this group and has a significant common Pb component.

Fifteen of the 16 analyses can be combined as a statistically coherent group, for which a weighted mean $^{206}Pb/^{238}U$ age of 526±5 Ma has been calculated (χ^2 = 0.72). The single analysis excluded from this calculation (6.1, Table 2) appears to have suffered Pb-loss. Combining the field and petrographic observations, the U-Pb SHRIMP age of 526±5 Ma is interpreted as the age of intrusion. The magmatic age obtained for the zircon from this granite is the youngest so far obtained for the granitoids of southern Ethiopia (cf. Table 1).

The mean ^{40}Ar-^{39}Ar age obtained from laser probe dating on biotite grains (Table 3) from the Metoarbasebat granite is 506±4 Ma and from hornblende it is 511±4 Ma. The age obtained from hornblende is preferred, as hornblende has better Ar retention properties than biotite (Guo and Dickin, 1996). This age is younger than the SHRIMP U-Pb zircon age (526±5 Ma) and could indicate the cooling age for the pluton.

Meleka Foliated Granodiorite

The Meleka foliated granodiorite occurs in the northernmost part of the Adola area (Fig.1, see also fig.3 of Yibas et al., 2000). This granodiorite is intrusive into the granite-gneisses of the western part of the Adola granite-gneiss complex, close to its contact with the Megado

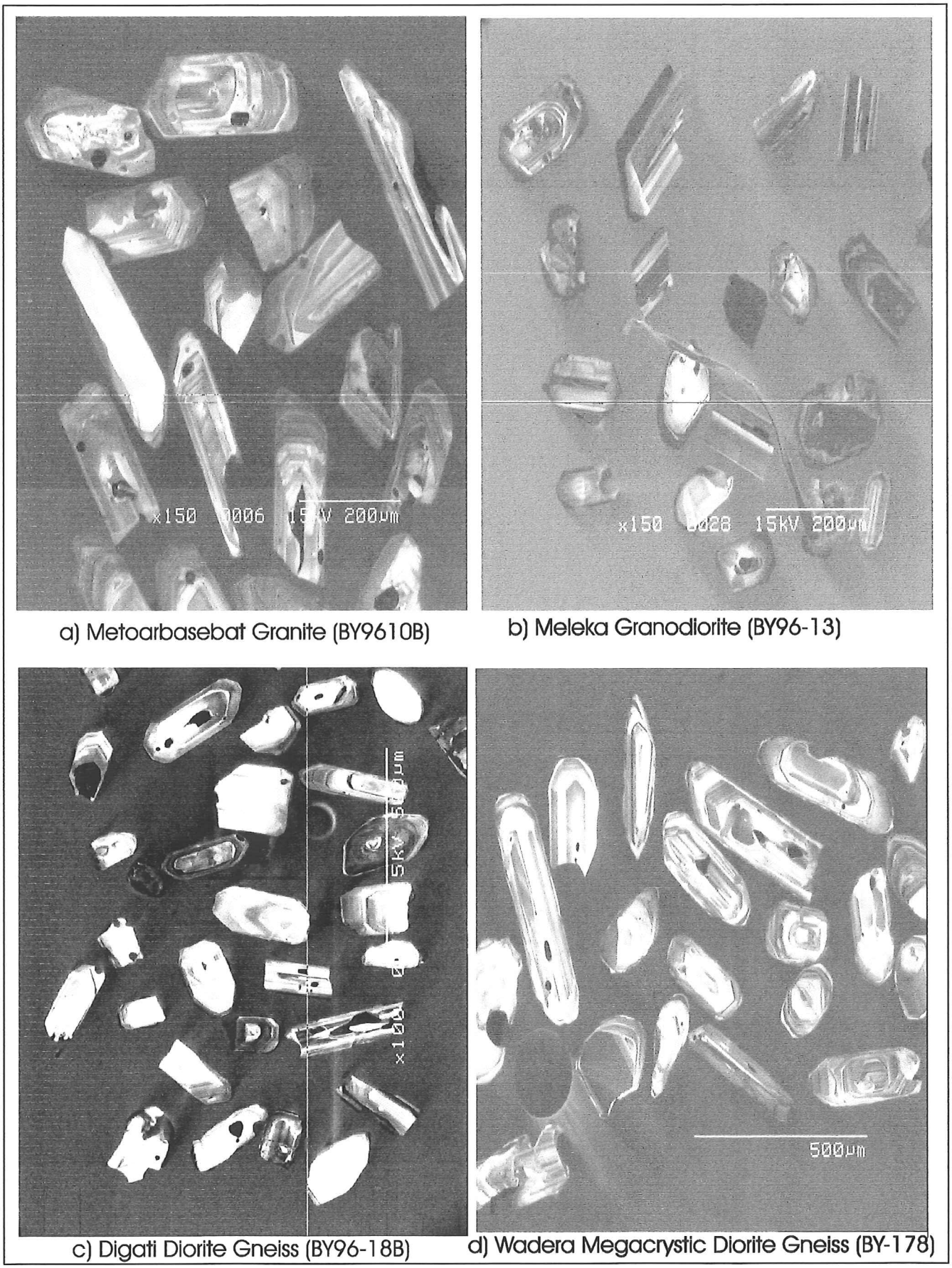

Figure 2: *Cathodoluminescence images of dated zircon grains from the granitoid rocks of the Precambrian of southern Ethiopia.*

Figure 2 (contd.)

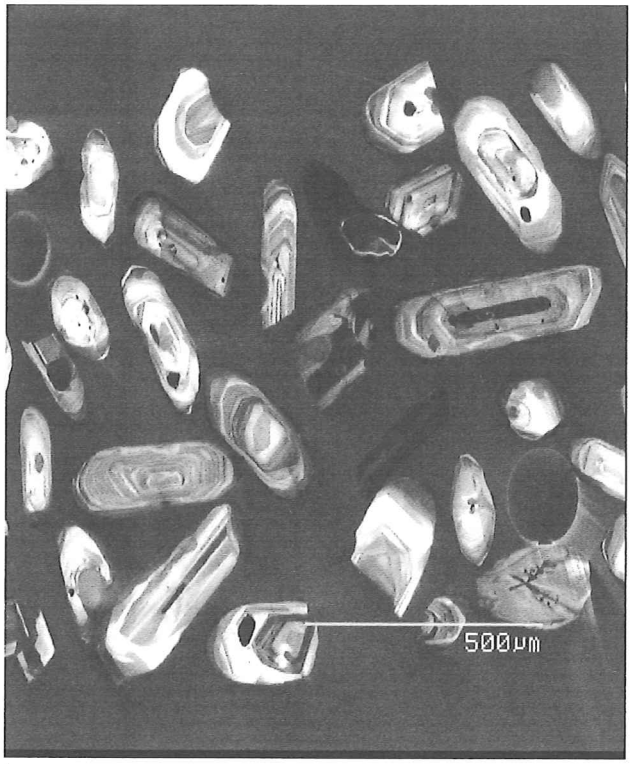

e) Wadera deformed granite dyke (BY-178-A).

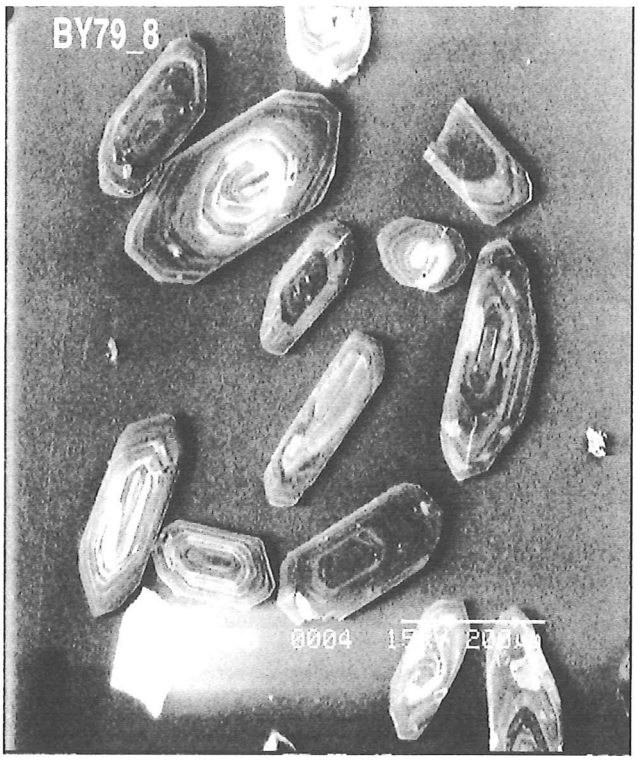

f) Moyale Granodiorite (BY-79).

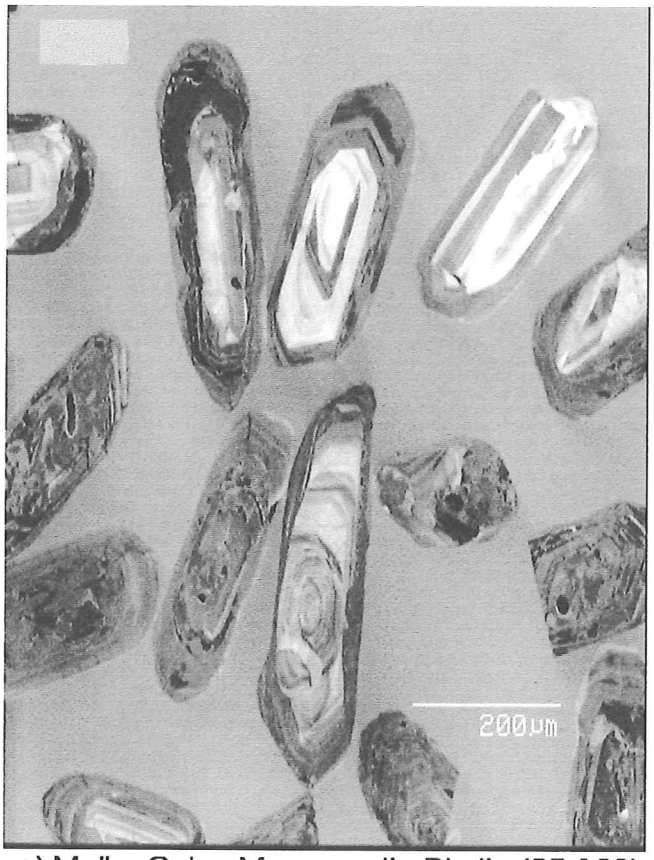

g) Melka Guba Megacrystic Diorite (97-183).

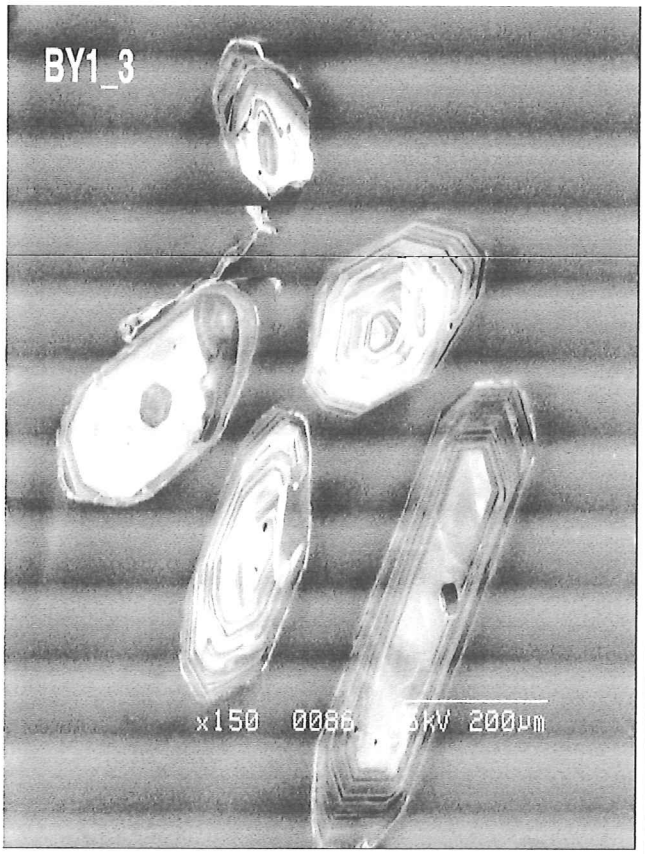

h) Bulbul Mylonitic Diorite Gneiss (96-81).

Belt (Fig. 1, see also fig.3 of Yibas et al., 2000). The Meleka granodiorite (sample BY96-13A) is composed of K-feldspar, plagioclase, quartz, and minor amounts of muscovite and biotite. It is weakly foliated and shows subtle compositional layering defined by grey and pink layers. The foliation strikes NNE-SSW. Aggregates of sulphide minerals and ovoids are stretched in NE-SW direction on slip planes and indicate that the rock has been subjected to deformation.

Table 2. Summary of SHRIMP U-Pb zircon results for granitoids of the Precambrian of southern Ethiopia

Grain spot	U	Th	Th/U	Pb*	$^{204}Pb/^{206}Pb$	f_{206} (%)	Radiogenic		Age (Ma)	
							$^{206}Pb/^{238}U$	±	$^{206}Pb/^{238}U$	±
Sample BY96-10B from the Metoarbasebat Granite, northwest of Moyale town										
1.1	315	131	0.42	26	0.000465	0.375	0.082	0.0039	506	23
2.1	265	100	0.38	23	0.000378	0.483	0.084	0.0014	523	8
3.1	224	124	0.55	20	0.000196	0.281	0.086	0.0011	531	7
4.1	311	110	0.35	27	0.000476	0.306	0.087	0.0011	536	7
5.1	168	123	0.73	14	0.000527	1.081	0.076	0.0016	474	10
6.1	34	24	0.70	3	0.002475	4.094	0.084	0.0019	523	11
7.1	312	55	0.18	26	0.000148	-	0.086	0.0014	534	8
7.2	34	18	0.54	3	0.000831	0.919	0.084	0.0023	520	14
8.1	99	43	0.43	9	0.000148	0.228	0.085	0.0017	528	10
9.1	261	95	0.37	23	0.000349	0.335	0.086	0.0012	535	7
10.1	253	102	0.40	22	0.000344	0.384	0.084	0.0011	520	7
11.1	256	95	0.37	22	0.000394	0.269	0.084	0.0011	520	7
12.1	73	44	0.59	7	0.000648	1.004	0.083	0.0018	513	10
13.1	299	101	0.34	26	0.000205	0.090	0.085	0.0011	526	6
14.1	253	46	0.18	21	0.000128	-	0.084	0.0013	521	7
15.1	145	70	0.48	13	0.000472	0.492	0.085	0.0012	525	7
Sample BY96-13A from the Meleka Granodiorite, northwest of the Adola Granite-Gneiss Complex.										
1.1	259	251	0.97	25	0.002471	5.29	0.0832	0.0023	515	14
1.2	4140	900	0.22	55	0.028255	50.3	0.0128	0.0006	82	4
2.1	400	404	1.01	47	0.000220	0.32	0.1004	0.0015	617	9
3.1	204	154	0.75	23	0.000381	0.6	0.1003	0.0013	616	8
4.1	777	310	0.40	71	0.003047	5.05	0.0899	0.0011	555	7
5.1	77	25	0.33	7	0.001717	2.6	0.0916	0.0014	565	8
6.1	588	168	0.29	48	0.002619	4.07	0.0820	0.0014	508	8
7.1	123	75	0.61	15	0.002633	4.81	0.1151	0.0022	702	13
8.1	259	254	0.98	17	0.010832	19	0.0573	0.0010	359	6
9.1	123	69	0.57	10	0.007849	13.9	0.0788	0.0018	489	11
9.2	580	80	0.14	49	0.000351	0.62	0.0897	0.0015	553	9
10.1	268	116	0.43	29	0.006025	13.8	0.1043	0.0055	639	32
11.1	244	159	0.65	26	0.020009	32.8	0.0982	0.0018	604	11
12.1	123	48	0.39	12	0.001634	2.72	0.0967	0.0020	595	12
13.1	613	1394	2.27	86	0.000197	0.2	0.0927	0.0016	572	9
14.1	190	146	077	21	0.000834	1.42	0.0979	0.0019	602	11
15.1	159	89	0.56	15	0.001332	2.49	0.0904	0.0016	558	9

Note: Uncertainties given at the one σ level; f_{206} % denotes the percentage of ^{206}Pb that is common Pb; – denotes no common Pb detected; correction for common Pb made using the measured $^{238}U/^{206}Pb$ and $^{207}Pb/^{206}Pb$ ratios following Tera and Wasserburg (1972), as outlined in Compston et al. (1992).

Table 2. (Contd.)

Grain spot	U	Th	Th/U	Pb*	$^{204}Pb/^{206}Pb$	f_{206} (%)	Radiogenic		Age (Ma)	
							$^{206}Pb/^{238}U$	±	$^{206}Pb/^{238}U$	±
Sample BY96-18B from the Digati Diorite Gneiss, southern part of the Megado Belt.										
1.1	114	110	0.96	13	0.000343	0.47	0.0938	0.0019	578	11
2.1	65	102	1.56	8	0.001312	1.17	0.0925	0.0019	570	11
3.1	279	32	0.11	27	0.000238	0.55	0.1035	0.0018	635	11
4.1	144	135	0.93	16	0.000386	0.059	0.0939	0.0017	578	10
5.1	127	203	1.59	16	0.000858	1.06	0.0917	0.0017	566	10
6.1	54	75	1.38	6	0.001765	4.20	0.0905	0.0020	558	12
7.1	101	152	1.51	12	0.000312	1.02	0.0926	0.0018	571	11
7.2	547	40	0.07	44	0.000133	0.20	0.0856	0.0053	529	31
8.1	59	77	1.30	7	0.001872	2.82	0.0965	0.0022	594	13
9.1	185	179	0.97	19	0.000340	0.38	0.8884	0.0016	566	9
10.1	135	115	0.85	14	0.000703	0.96	0.0918	0.0016	566	10
11.1	122	113	0.92	13	0.001036	1.05	0.0908	0.0017	560	10
12.1	107	101	0.95	11	0.001203	1.47	0.0920	0.0017	567	10
13.1	175	169	0.97	16	0.000484	0.93	0.0779	0.0029	483	17
14.1	85	79	0.93	8	0.000386	2.81	0.0745	0.0048	463	29
Sample BY96-178 from the Wadera Megacrystic Diorite Gneiss, Wadera Shear Zone										
1.1	481	78	0.16	41	0.000370	0.10	0.0897	0.0011	554	6
1.2	102	78	0.77	11	0.001623	0.45	0.0926	0.0016	571	9
2.1	123	133	1.08	13	0.000073	0.25	0.0923	0.0018	569	10
3.1	83	134	1.62	10	0.000634	0.32	0.0926	0.0015	571	9
3.2	179	130	0.73	17	0.000202	-	0.0848	0.0012	524	7
4.1	291	6	0.02	23	0.000063	-	0.0866	0.0011	535	7
5.1	551	444	0.81	59	0.000035	-	0.0957	0.0011	589	6
5.2	61	43	0.71	6	0.000155	0.37	0.0960	0.0018	591	11
6.1	136	119	0.87	15	0.000441	0.09	0.0936	0.0015	577	9
7.1	218	169	0.77	24	0.000010	0.11	0.0967	0.0012	595	7
8.1	138	122	0.88	15	0.000297	0.25	0.0938	0.0018	578	10
9.1	224	175	0.78	24	0.000202	0.04	0.0943	0.0013	581	7
10.1	124	112	0.90	13	0.000476	0.89	0.0917	0.0013	566	8
11.1	237	15	0.06	21	0.000106	0.11	0.0934	0.0012	575	7
11.2	92	89	0.96	10	0.000010	0.42	0.0949	0.0017	584	10
11.3	40	37	0.92	4	0.001384	1.02	0.0910	0.0020	561	12
12.1	142	63	0.44	13	0.000354	0.43	0.0884	0.0015	546	9
12.2	38	56	1.46	5	0.000136	1.13	0.0928	0.0019	572	11
Sample BY96-178A from a granitic dyke crosscutting the Wadera Megacrystic Diorite Gneiss, Wadera Shear Zone										
1.1	357	287	0.81	38	0.000235	0.20	0.0940	0.0016	579	10
2.1	182	142	0.78	19	0.000179	0.59	0.0922	0.0016	568	10
3.1	203	162	0.80	21	0.000642	0.22	0.0929	0.0017	572	10
4.1	224	175	0.78	24	0.000322	0.40	0.0935	0.0019	576	11
5.1	163	140	0.85	18	0.000367	-	0.0985	0.0020	606	12
6.1	171	144	0.84	18	0.000153	0.45	0.0936	0.0018	577	11
7.1	156	97	0.62	16	0.000736	0.86	0.0960	0.0020	591	12
8.1	151	157	1.04	17	0.000010	0.45	0.0962	0.0018	592	11
9.1	186	149	0.80	19	0.000282	0.63	0.0898	0.0018	554	11
10.1	44	41	0.92	5	0.000269	3.89	0.0914	0.0028	564	17
10.2	286	238	0.83	30	0.000212	-	0.0924	0.0017	570	10
11.1	198	82	0.42	19	0.000247	0.41	0.0938	0.0020	578	12
12.1	71	62	0.88	7	0.001083	2.01	0.0833	0.0250	516	151
13.1	168	127	0.76	16	0.000635	0.61	0.0858	0.0018	531	10

Table 2. (Contd.)

Grain spot	U (ppm)	Th (ppm)	Th/U	Pb* (ppm)	$^{204}Pb/^{206}Pb$	f_{206} (%)	Radiogenic		Age (Ma)	
							$^{206}Pb/^{238}U$	±	$^{206}Pb/^{238}U$	±
Sample BY96-79 from the Moyale Granodiorite, central part of the Moyale Belt, southern Ethiopia.										
1.1	283	68	0.24	29	0.000268	0.39	0.1064	0.0013	652	8
1.2	756	115	0.15	79	0.000049	0.21	0.1093	0.0012	669	7
2.1	487	97	0.20	52	0.000026	0.09	0.1099	0.0012	672	7
3.1	442	133	0.30	47	0.000049	0.07	0.1084	0.0012	663	7
4.1	856	200	0.23	81	0.000776	1.36	0.0969	0.0011	596	6
4.2	463	98	0.21	50	0.000035	0.09	0.1106	0.0013	676	7
5.1	496	122	0.25	51	0.000201	0.34	0.1048	0.0012	643	7
6.1	1035	186	0.18	101	0.000643	1.19	0.1015	0.0011	623	6
7.1	1375	207	0.15	143	0.000251	0.47	0.1089	0.0012	667	7
7.2	380	172	0.45	43	0.000016	0.14	0.1098	0.0013	672	8
8.1	283	131	0.46	32	0.000169	0.13	0.1098	0.0015	672	9
9.1	846	359	0.42	92	0.000156	0.30	0.1057	0.0012	648	7
10.1	1062	186	0.17	111	0.000134	0.31	0.1088	0.0011	666	7
11.1	932	179	0.19	0.92	0.000224	0.51	0.1024	0.0011	628	7
12.1	909	92	0.10	94	0.000108	0.31	0.1098	0.0012	672	7

Table 2. Continued.

Grain spot	U (ppm)	Th (ppm)	Th/U	Pb* (ppm)	$^{204}Pb/^{206}Pb$	f_{206} (%)	±	Radiogenic		Age (Ma)	
								$^{206}Pb/^{238}U$	±	$^{206}Pb/^{238}U$	±
Sample BY97-81 from the Bulbul Mylonitic Diorite Gneiss, Bulbul Belt.											
1.1	349	27	0.08	49	0.000016	0.45	0.00178	0.1515	0.0018	910	10
1.2	405	50	0.12	55	0.000060	0.38	0.00164	0.1452	0.0016	874	9
1.3	89	34	0.38	13	0.000156	0.64	0.00189	0.1388	0.0019	838	11
2.1	89	75	0.84	15	0.000215	0.78	0.00201	0.1448	0.0020	872	11
3.1	577	405	0.70	56	0.003061	5.31	0.00109	0.0903	0.0011	557	6
4.1	255	77	0.30	37	0.000096	0.32	0.00171	0.1454	0.0017	875	10
5.1	246	116	0.47	37	0.000069	0.42	0.00182	0.1465	0.0018	881	10
6.1	468	231	0.49	67	0.000079	0.50	0.0016	0.1388	0.0016	838	9
7.1	139	50	0.36	20	0.000081	0.30	0.00827	0.1410	0.0083	850	47
8.1	556	229	0.41	83	0.000045	0.30	0.00162	0.1459	0.0016	878	9
9.1	57	44	0.77	9	0.000370	0.44	0.0027	0.1481	0.0027	890	15
10.1	723	322	0.44	107	0.000018	0.30	0.00151	0.1439	0.0015	866	9
11.1	182	103	0.57	28	0.000214	0.52	0.00173	0.1451	0.0017	874	10
12.1	134	81	0.61	21	0.000185	0.37	0.00194	0.1469	0.0019	883	11

The heterogeneity of the zircon population the Meleka granodiorite, which can be seen in Figure 2b, is also reflected in the complexity of the chronological results and the widely divergent U and Th contents and U/Th ratios derived from the SHRIMP analyses (Table 2). Seventeen analyses on 15 different grains were carried out. The results are presented in Table 2 and are plotted, uncorrected for common Pb, on a Tera-Wasserburg U-Pb concordia diagram (Fig. 3b). Two main observations can be made from this plot: (1) the high common Pb contents of some of the zircons; and (2) the considerable spread of ages for the zircons analysed. Some of this complexity undoubtedly results from radiogenic Pb-loss (e.g., analysis 1.2 from a rim, Table 2), where extremely high U concentrations (up to 4140 ppm) have resulted in extensive radioactive damage. This produces apparent ages, which are seemingly

too young. A number of analyses also plot to the left of the main group, which indicates the presence of older, inherited components.

Clearly, it is very difficult to interpret the age data for the zircons from this sample, and the identification of a single magmatic age, which would give the age of emplacement, is subjective. It is possible, based on a statistical assessment of the data, to define three groups of ages, which might each represent a magmatic event. The older group (Age I) gives a weighted mean $^{206}Pb/^{238}U$ age of 610±9 Ma, and Age II gives a weighted mean $^{206}Pb/^{238}U$ age of 560±8 Ma. Three of the analyses for this sample represent a much younger age group (Age III) with ages between 489 and 515 Ma (compare Table 2, not given in Fig. 3b).

The ^{40}Ar-^{39}Ar ages from the biotite grains gave two groups of ages: the oldest and the youngest mean ages are 534.5±8 and 512±4 Ma, respectively. The muscovite grains, however, gave a mean age of 515±3 Ma, similar to the youngest age obtained from the biotite.

When these ^{40}Ar-^{39}Ar ages are compared with the SHRIMP data the following useful correlation can be made:

(1) Age III (489 to 515 Ma) represents the youngest SHRIMP data for the Meleka foliated granodiorite and is similar to the ages obtained for the Metoarbasebat granite - the youngest granite in the study area. The ^{40}Ar-^{39}Ar ages obtained from both granites are also similar. This suggests that this age group represents the youngest tectonothermal and magmatic event to have occurred in the region;

(2) Age II of 560±8 Ma is correlative with the emplacement age of the Digati diorite gneiss (cf. below); and

(3) Age I (610±9 Ma) is, therefore, the most likely age for the emplacement of the Meleka granodiorite.

An inherited zircon gave a 700 Ma age (analysis 7.1, Table 2).This correlates well with the age of emplacement of the Moyale ophiolitic amphibolite, as constrained by U-Pb zircon ages dated by Teklay et al. (1998).

Digati Diorite Gneiss

The Digati diorite gneiss (Sample BY96-18B) occurs along the western tectonic boundary between the Megado ophiolitic fold and thrust belt and the western Gneissic Domain of Adola (Fig. 1). It is well foliated, banded, and composed of feldspars, quartz, amphibole, biotite and garnet. The garnet porphyroblasts contain inclusion trails, probably of earlier S-surfaces. Two generations of biotite are evident in thin section. The earlier generation defines the foliation together with quartz and feldspar grains, whereas the younger biotites clearly post-date the foliation and occur at random, sometimes forming knots.

Basic dykes intruded the Digati diorite gneiss concordant to the gneissic foliation. These basic dykes are fine-grained, dark-grey, and well foliated, and are composed mainly of amphibole and plagioclase. The basic dykes are, in turn, intruded by felsic veinlets, which are tightly folded parallel to the foliation.

Mineralogical studies of the zircon grains from the sample collected from the Digati diorite gneiss show the presence of different populations of zircon both in terms of their size and

morphology (Fig. 2c). The dominant zircon grains are translucent to cloudy and long to short prismatic, with rounded to sub-rounded to bipyramidal bases. Some of the long prismatic grains with bipyramidal faces show fractures.

Fifteen SHRIMP U-Pb zircon analyses were made on 14 different zircon grains from the Digati diorite gneiss (Table 2). Most of the analyses plot as a coherent group, but a number of data scatter around it (Fig. 3). The main group of data yields a weighted mean $^{206}Pb/^{238}U$ age of 570±7 Ma. Those analyses, which fall outside of this group, include:

(1) one analysis (3.1, Table 2, Fig. 3c),which is significantly older (635±11Ma), indicating inheritance from an older crustal component; (2) several zircons (9.1, 13.1 and 14.1) which have obviously lost radiogenic Pb (i.e. are discordant); and (3) a single analysis of a complex

Table 3. Laser probe $^{40}Ar/^{39}Ar$ dating results for single mineral grains from Precambrian rocks in southern Ethiopia (N = number of analysed points per sample)

Locality	Sample No.	Rock type	Mineral	Grain No.	Analysis position	Age	Mean Age (Ma)
Lega Dembi Gold Deposit	LG96-8A	Quartz vein	Muscovite	BY1-1	rim	514 ± 7	516 ± 3 (N =5)
					core	536 ± 7	
				BY1-2	rim	515 ± 7	
					core	512 ± 8	
				BY1-3	Rim	515 + 7	
					core	522 ± 7	
NW of Moyale Town	BY96-10B	Metoarbasebat Granite	Biotite	BY2-1	rim	493 ± 7	506 ± 4 (N = 5
					core	504 ± 7	
				BY2-2	Rim	510 ± 7	
					Core	501 ± 7	
				BY2-3	Rim	511 ± 7	
					Core	502 ± 10	
			Hornblende	BY2-4	Rim	505 ± 9	511 ± 4 (N = 3)
					Core	515 ± 16	
				BY2-5	Rim	513 ± 8	
					core	462 ± 21	
Northern Adola	BY96-13A	Meleka Foliated Granodiorite	Biotite	BY3-1	Rim	540 ± 7	512 ± 4 (N = 4)
					Core	529 ± 9	
				BY3-2	Rim	515 ± 6	
					Core	512 ± 6	
				BY3-3	Rim	512 ± 6	
					Core	505 ± 9	
			Muscovite	BY3-4	Rim	512 ± 6	515 ± 3 (N = 4)
					Core	491 ± 12	
				BY3-5	fusion	512 ± 7	
Southern Megado Belt (Digati)	BY96-18B	Digati Diorite Gneiss	Biotite	BY4-1	Rim	506 ± 5	502 ± 4 (N = 4)
					core	496 ± 5	
				BY4-2	Rim	503± 5	
					Core	502 ± 5	
Bulbul Belt	BY96-81	Bulbul Diorite Mylonite Gneiss	Biotite	BY5-1	Rim	514 ± 6	495 ± 5 (N = 4)
					Core	511 ± 6	
				BY5-2	Rim	484 ± 5	
					Core	475 ± 4	
				BY5-3	Rim	491 ± 5	
				BY5-4	Core	421 ± 4	

zircon (7.2) from an area which had been identified through cathodoluminescence imaging as an embayment structure (Fig. 2). This new zircon growth post-dates the main phase of (magmatic) growth and also has a very much lower Th/U ratio than the older zircon. This latter feature is a commonly observed characteristic of metamorphic zircon; hence, this analysis was excluded from the final age calculation above. The age of 529±31 Ma obtained for this growth phase is, however, not significantly different from the age calculated for the main magmatic growth (570±7 Ma), and hence, it can be concluded that there might not have been much time between magmatism and metamorphism.

The ^{40}Ar-^{39}Ar laser dating on biotite grains gave a mean age of 502±4 Ma (Table 3). The core of the biotite grains gave younger ages than the rims. The single SHRIMP result of 529±31 Ma obtained on late zircon growth overlaps within error limits with this ^{40}Ar-^{39}Ar age. This age is interpreted as a metamorphic age for the Digati diorite gneiss.

Wadera Megacrystic Diorite Gneiss

The mylonitic Wadera diorite gneiss (sample BY97-178) is coarse-grained with megacrystic K-feldspar grains. It is composed of quartz, K-feldspar, plagioclase, amphibole, and biotite. The megacrysts were modified by deformation and impose an augen (flaser) texture onto the rock. This rock intruded concordantly into the amphibole-gneiss of the Genale-Dolo Granite-Gneiss Complex. The megacrystic diorite gneiss has been intruded later by a series of granitic dykes, discordant to the pervasive foliation in the gneiss; both rock types were deformed together. Two main zircon populations were separated from the sample collected from the Wadera megacrystic diorite gneiss (Fig. 2d). Population 1 is dominated by long to medium-grained prismatic zircon grains, with rounded terminations (less prominent pyramidal faces), that are smoky yellow or transparent in colour. A few grains with relatively well-developed pyramidal faces were also observed in this group. Population 2 is characterised by fine-grained zircon crystals that are dominated by oval to round shapes of probable metamorphic origin.

The U-Pb SHRIMP data for this sample (Table 2) are plotted on a Tera-Wasserburg diagram in Figure 3d. There is a well-constrained group of data points near the concordia curve, but also some evidence of Pb-loss in four of the analyses, which are spread out to the right of the main group, giving relatively younger apparent $^{206}Pb/^{238}U$ ages. The main group of data gives a weighted mean $^{206}Pb/^{238}U$ age of 579±5 Ma (χ^2 = 1.38; N = 14). Three of the analyses, which gave younger ages of 546-524 Ma (and which were excluded from the age calculated above), are of rims or overgrowths of zoned grains and represent younger zircon growth (Fig. 3d). The 579±5 age is slightly older than the SHRIMP U-Pb age of 575±5 Ma obtained for the Wadera granite dyke, which is intrusive into the diorite gneiss (cf. below).

Wadera Deformed Granitic Dyke

A foliated granitic dyke (sample BY97-178A) intruded the Wadera megacrystic diorite gneiss discordantly to the foliation. The dyke is composed of quartz, K-feldspar, and plagioclase (strongly altered to epidote group minerals), besides accessory biotite and sphene. The zircon population of the sample from this dyke is dominated by rounded to subrounded, short prismatic crystals, when compared with the zircons of the diorite gneiss (Fig. 2e). The SHRIMP U-Pb analyses for the zircons from the Wadera granitic dyke sample are listed in Table 2 and plotted in Figure 3e. Apart from one analysis (13.1, Table 2), which suggests that

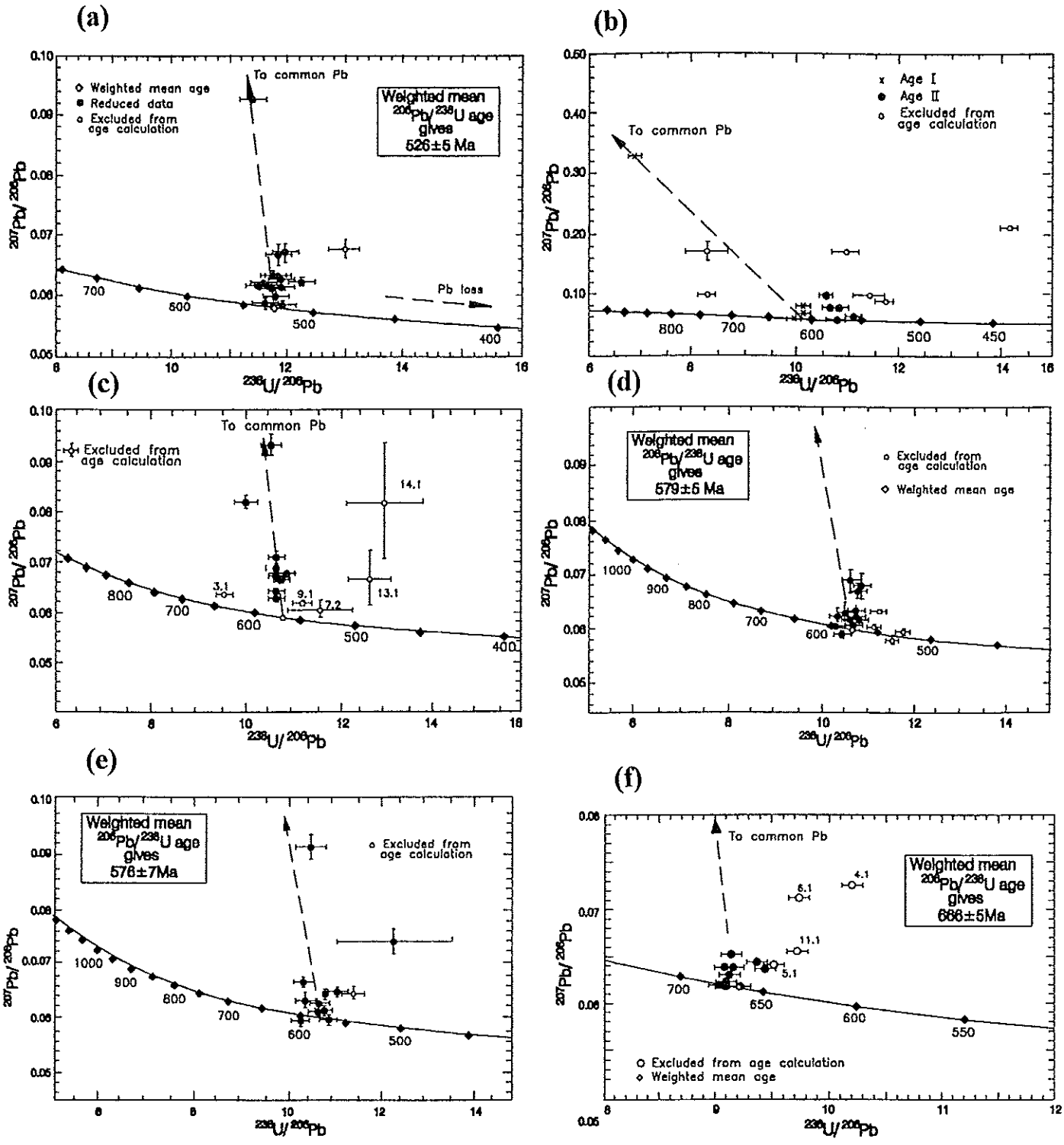

Figure 3: (a) to (g) and (j) are Tera-Wasserburg U-Pb concordia plots of SHRIMP data (uncorrected for common Pb) for samples from granitoids of southern Ethiopia. (h) is a conventional (Wetherill) U-Pb plot and (i) is a Th/U versus age plot for the two main groups of SHRIMP age data for sample BY 97183 from the Melka Guba megacrystic diorite gneiss.

Figure 3 (Contd.)

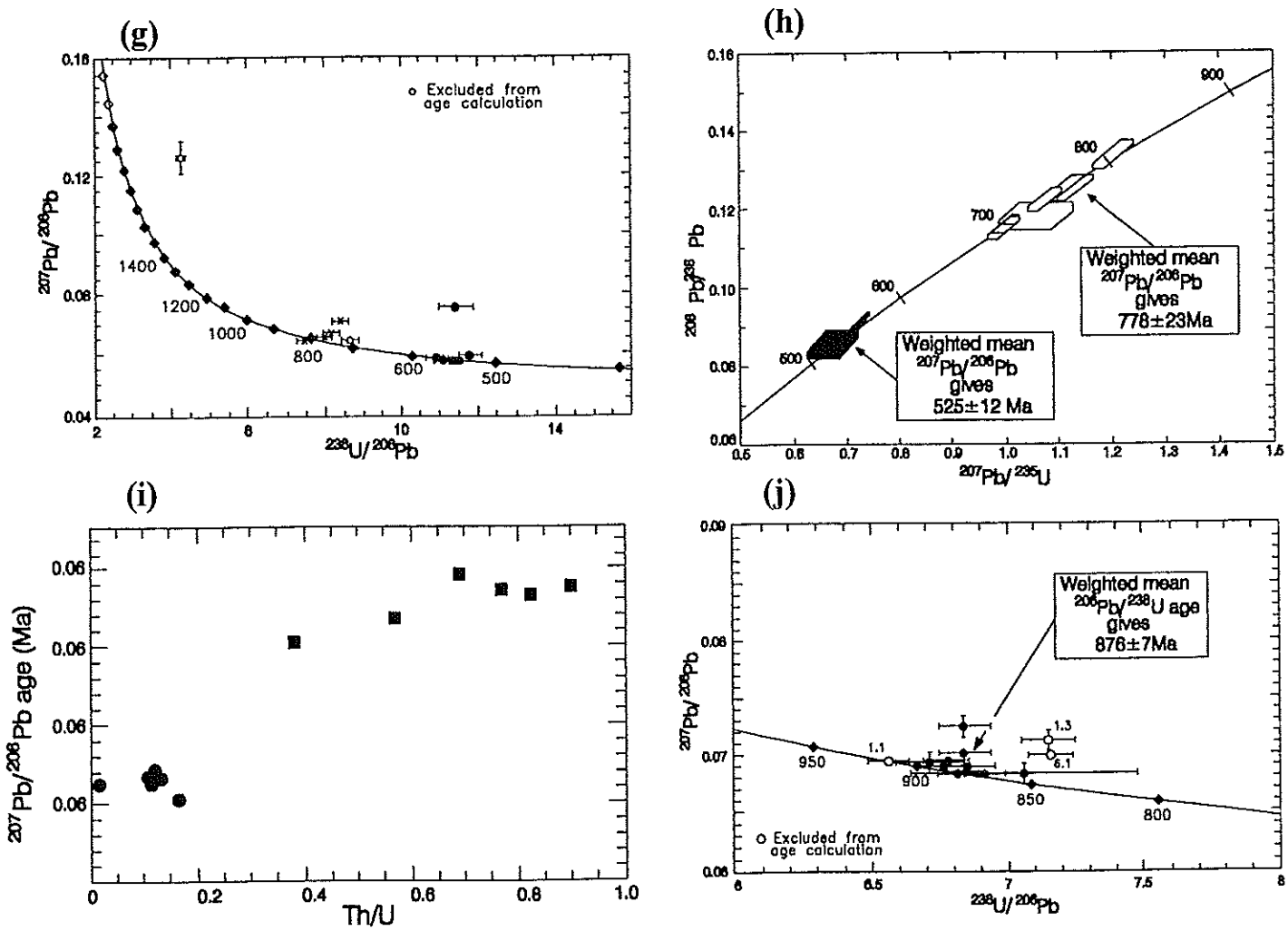

this grain has suffered Pb-loss, all data can be combined to produce a well-defined weighted mean $^{206}Pb/^{238}U$ age of 576±7 Ma (χ^2 = 1.31). This age is interpreted to be the magmatic age for the granite dyke.

Moyale Granodiorite

The Moyale granodiorite (sample BY97-79) occurs as a NW-SE trending body in and around Moyale town. This granodiorite intruded the Moyale fold and thrust sub-belt, as witnessed by the nature of its contact with the migmatised amphibole gneiss to the west and amphibolites to the east (Fig. 1). Along and near the contact of this unit, xenoliths of amphibolites are common. Plagioclase, quartz, and K-feldspar are the dominant minerals in the granodiorite, with minor to trace amounts of biotite, clinozoisite, epidote, sphene, apatite and chlorite.

The zircon population of the Moyale granodiorite is relatively homogeneous in that the dominant population is characterised by long prismatic forms. Some of the grains are slightly rounded, transparent to translucent crystals, with a subordinate amount of short prismatic grains (Fig. 2f).

Apart from variable degrees of Pb-loss in a number of zircon grains analysed, the zircons from this sample appear to belong to a relatively simple, probably magmatic population. The U-Pb data for 15 analyses on 12 different zircon crystals are presented in Table 2 and are plotted on a Tera-Wasserburg concordia plot in Figure 3f. Eleven of the analyses define a statistically robust group with a weighted mean $^{206}Pb/^{238}U$ age of 666±5 Ma (χ^2 = 1.49). The weighted mean $^{207}Pb/^{206}Pb$ age for all analyses gives a less precise date of 669±10 Ma (χ^2 = 1.03; N=15), but this age is in excellent agreement with the $^{206}Pb/^{238}U$ age and is regarded as the age of magmatism of the granodiorite. Teklay et al. (1998) obtained a 657.9±0.8 Ma single zircon $^{207}Pb/^{206}Pb$ evaporation age for a sample from the Moyale granodiorite, which is also in good agreement with the results reported here.

Melka Guba Megacrystic Dioritic Gneiss

The Melka Guba megacrystic diorite gneiss (sample BY97-183) occurs in the southwestern-most part of the Genale-Dolo Granite-Gneiss Complex (Fig. 1) close to the Melka Guba Bridge crossing the Dawa River. The diorite gneiss is mainly composed of amphibole, feldspar and quartz, and is well banded with prominent K-feldspar augen. It is strongly deformed with characteristic hook folds and transpositional gneissic layering.

Mineralogical studies of the zircon grains (Fig. 2g) extracted from this sample show the presence of different populations of zircon grains, in terms of both size and morphology:

(1) size fraction < 90 μm. This size fraction could be classified into two populations: Population 1 is dominated by cloudy and long-prismatic zircon grains, which have retained their bipyramidal base. A few acicular, smoky brown grains with slightly to moderately rounded bipyramidal bases were also observed in this group. Population 2 is dominated by light-coloured, less cloudy to translucent (a few smoky), and rounded to oval-shaped (metamorphic?) zircon grains;

(2) size fraction 125 to 90 μm. This size fraction also shows two distinct populations. Population 1 is dominated by long, prismatic grains with rounded bipyramidal faces. Most grains are fractured, non-translucent to smoky, and a few grains are brownish. Population 2 comprises zircon grains, which are oval or round in shape. A few of these grains show new growth of zircon on one of their tips. A few corroded zircon grains might represent a third, but smaller population.

(3) size fraction 250-125μm. Most zircon grains are smoky brown in colour and can be grouped into two major populations. Population 1 is dominated by long- to short- prismatic zircon grains with rounded to semi-rounded bipyramidal bases. Some of these grains show corrosion and/or fracturing. A few of these zircon grains are long-prismatic, smoky brown, and well faceted. These grains show characteristic zoning with a translucent core, but with opaque inclusions. The zircon grains in Population 2 are dominated by oval to rounded and translucent grains. A few grains from Population 2 are strongly corroded.

(4) >250 μm size fraction. Except for their grain sizes, the zircon grains of this size fraction have the same populations described in (3).

The cathodoluminescence images for the complex zircon population (Fig. 2g) and the actual SHRIMP data, as presented in Table 2 and Figure 3g, show the structural complexity of the zircons classified above. Clearly, there are at least three age populations (Fig. 3g). The oldest

groups of analyses plot near to the concordia (Figs. 3g,h), with the older group showing some spread suggesting either Pb-loss or a genuine range in ages. A weighted mean $^{207}Pb/^{206}Pb$ age of 778±23 Ma can be calculated from five of the six analyses within this group, but the spread in U-Pb ratios (Fig. 3i) precludes the calculation of any meaningful $^{206}Pb/^{238}U$ age for these data. The other group also shows some spread in U-Pb ratios, but all six analyses combine to give a weighted mean $^{207}Pb/^{206}Pb$ age of 525±12 Ma (Fig. 3h).

The different age groups described can generally be matched to morphology, but not in every case. For example, the zircons analysed from the *c.* 778 Ma group are generally core analyses, but some are from outer zones.

There is, however, a definite difference in chemical composition between the grains from the two age groups, with a significant difference in Th/U ratios (Fig. 3i). The lower Th/U ratios of the younger phase of zircon growth could be indicative of a metamorphic origin for this zircon (Tera and Wasserburg, 1972). The geological relationships and metamorphic history of the rock clearly indicate that the 778±23 Ma age is the age of emplacement.

The individual age data (Table 2) can be resolved into three age groups: 807±20 Ma (1 analysis), 752.6±18.6 (3 analyses) and 710±18 (2 analyses). The *c.* 807 Ma age can be regarded as another xenocryst from the core of an inherited crystal (the rim of which was dated at 532±20 Ma). The 756.6 Ma age, by contrast, can be regarded as the emplacement age of the megacrystic diorite, from which the gneiss evolved by metamorphism that must have occurred at 710±18 Ma. If this interpretation is correct, it follows that these magmatic and metamorphic events occurred within a narrow time interval. The youngest age group can also be resolved into 552±13.25 Ma and 529±16.5 Ma age subgroups, which are correlative with the Digati and Metoarbasebat granite emplacement ages, respectively.

Bulbul Mylonitic Diorite Gneiss

The Bulbul mylonitic diorite gneiss (sample BY 96-81) occurs in the Bulbul Shear Zone sandwiched between the western and eastern parts of the Bulbul mafic-ultramafic belt (Fig. 1; see also fig. 3 of Yibas et al., 2000). The gneiss is coarse-grained, grey, strongly sheared and well foliated. It is composed of plagioclase, quartz, amphibole, brown biotite, and accessory sphene and zircon. It is characterised by ophitic feldspars rotated during the development of the N-S trending mylonitic fabric. Kazmin (1972, 1975) mapped the mylonitic diorite gneisses as the Burji Gneiss of the Lower Complex (the latter regarded by him as Archaean in age).

As with many of the samples dealt with in this project, the SHRIMP analyses on zircons from the Bulbul diorite gneiss show that there is significant complexity and heterogeneity within the individual zircon separates. Two dominant zircon populations were identified: one that comprises long-prismatic crystals, with rounded to semi-rounded bases, and another, which is dominated by short-prismatic grains, with rounded to semi-rounded bases (Fig. 2h).

The SHRIMP data for this sample are plotted on a Tera-Wasserburg concordia diagram (Fig. 3 j). The majority of the data points plot as a group near the concordia curve. For this group, a $^{206}Pb/^{238}U$ age of 876±7 Ma can be calculated ($\chi^2 = 0.39$; N=10). This would appear to be the magmatic age for this sample. Three analyses (1.3, 3.1 and 6.1) plot to the right of the main group and give lower apparent ages. Cathodoluminescence imaging showed that these analyses are not part of a younger overgrowth phase. Thus, it is concluded that these grains have most likely suffered Pb-loss. Analysis 1.1 is of a core in a zoned grain, which is

significantly older (910±10 Ma) than the outer overgrowth phase, which has the same age as the dominant population presumed to be magmatic in origin.

^{40}Ar-^{39}Ar laser dating on biotite grains gave a mean age of 495±5 Ma. This age represents the youngest tectonothermal event recognised to date in the study area.

DISCUSSION

Granitic Magmatism in the Precambrian of Southern Ethiopia

The combined use of SHRIMP and $^{40}Ar/^{39}Ar$ dating techniques helped considerably to decipher the sequence of major magmatic and tectonothermal events that affected the study area during the period between ~ 900 and 500 Ma. The granitic magmatism of southern Ethiopia, which occurred during the East African orogeny, can be subdivided into 7 major magmatic events (Table 4). The geochronological data discussed above and field studies (Yibas, 2000; Yibas et al., 2000) of the various granitoids permitted classification of the granitoids into seven groups. These include: Gt1 (>880 Ma), Gt2 (800-770 Ma), Gt3 (770-720 Ma), Gt4 (720-700 Ma), Gt5 (700-600 Ma), Gt6 (580-550 Ma), and Gt7 (550-500 Ma) (Table 4 and fig. 3 of Yibas et al., 2000).

In general, the age data from selected granitoids of the Precambrian of southern Ethiopia show similarity to the Pan-African ages obtained from the granitoids of the western Ethiopian Precambrian terrane (~830 to 540 Ma - Ayalew et al., 1990). It is also evident that the dominant granitic magmatism in the area occurred during the period between ~750 and 500 Ma, with only 10 out of 42 samples showing ages older than 750 Ma (Fig. 4). Pre-Pan African ages are recognised from zircon xenocrysts contained in some of the granitoids of southern Ethiopia (e.g., the Melka Guba diorite gneiss, from which xenocryst SHRIMP ages ranging from 2050 to 1362 Ma were obtained - this study). Teklay et al. (1997, 1998) also obtained ages of 1125±2.5 and 1656.8±1.9 Ma (single zircon evaporation technique) for xenocrystic zircon from a metarhyolite from southern Ethiopia. These xenocryst ages strongly indicate the presence of Palaeo- to Meso-Proterozoic continental crust in the Precambrian of southern Ethiopia, which has been rejuvenated during the East African orogeny. Palaeoproterozoic to Archaean ages for xenocryst zircons were also found in the granitoid gneisses in northern Somalia (Kröner, 1993) and in eastern Ethiopia (Teklay et al., 1998). The granitoid gneisses in northern Somalia and southern Ethiopia, in which these older zircon xenocrysts were found, have similar magmatic ages ranging from 780 to 840 Ma. In the western part of the crystalline basement of northern Somalia, xenocrysts of Palaeoproterozoic age of ~1400 to ~1820 Ma in 720-840 Ma old granitoids have been reported (U-Pb single zircon evaporation; Kröner and Sassi, 1996). Such ages have not been reported to date from the western Ethiopian Precambrian terrane.

Basement rocks in the Buur area of southern Somalia include high-grade igneous and metasedimentary rocks of presumed Early Proterozoic to Archaean age (Haider, 1989), which are intruded by Pan-African granitoids (~470-550 Ma; 600-550 Ma - Lenoir and Haider, 1990; Lenoir et al., 1993). In the southwestern sector of the Buur Precambrian basement, granitoids are syn- to late-kinematic (600-550 Ma), whereas in the northeastern sector, they are essentially post-kinematic (470 Ma) (Lenoir et al., 1993). Lenoir et al. (1993) also showed that the granitoids in northern Somalia are older (630-550 Ma) and mainly of mantle origin. In the southern region of the country they are younger (550-470 Ma) and mainly of crustal origin indicating the presence of a transitional regime characterised in the north by a strong

subduction imprint, close to the Arabo-Nubian Shield. Intense crustal reworking prevailed in the south, which is consistent with the Mozambican continental collision (Lenoir et al., 1993).

Table 4. Geochronological classification of granitic magmatism in the Precambrian of southern Ethiopia during the East African Orogeny

Granitic phases/ages	Dated Granites	Age (Ma)	
		Zircons U-Pb	$^{40}Ar/^{39}Ar$ Laser
Gt7 [550-500 Ma]	Metoarbasebat granite	526± 5[β]	506 ± 4 (Bt); 511 ± 3 (Hb)
	Berguda charnockitic granite	528 ± 8.4[α] (rim) 538 ± 3[α](core)	
	Lega Dima granite	550 ± 18[γ]	
	Robele granite	554 ± 23[ε]	
Gt6 [550-600 Ma]	Wadera foliated granite	576 ± 5[β]	
	Wadera megacrystic diorite gneiss	579 ± 5[β]	
	Digati dioritic gneiss	570 ± 5[β]	502 ± 4 (Bt)
Gt5 [700-600 Ma]	Burjiji granitic massif	~602 Ma[γ]	
	Meleka foliated granodiorite	610 ± 9[β]	512 ± 4 (Bt), 515 ± 4 (Mu)
	Gariboro granite	~646[γ]	
	Moyale granodiorite	666 + 5[β]	
Gt4 [720-700 Ma]	Finchaa biotite-foliated granite	708 ± 5[ε]	
	Yabello charnockitic granite-gneiss	716 ± 5[τ]	
Gt3 [770 –720 Ma]	Alghe granite-gneiss	722 ± 2τ	
	Sagan basic charnockite	725[τ]	
	Zembaba granite-gneiss	756 ± 6[τ]	
	Sebeto tonalite gneiss	765 ± 3[ε]	
Gt2 [>770 Ma]	Melka Guba megacrystic granodiorite gneiss	778 ± 23[β]	
Gt1[>880 Ma]	Bulbul diorite mylonite	876 ± 7[β]	495 ± 5 (Bt)

β = this study; α Gichile(1999): γ Worku (1996); ε Genzebu et al.(1994); τ Teklay et al.(1993) (β = SHRIMP, U-Pb; all others = U-Pb single zircon evaporation method). Hb =hornblende, Bt = biotite, Mu = muscovite.

Tectonomagmatic Events, Metamorphism and Post Orogenic Cooling

The following tectonothermal sequence is proposed for the Precambrian of southern Ethiopia, based on the available geochronological data for granitoid emplacement and metamorphic episodes. Possible correlation of these tectonothermal events with those of the adjacent Pan-African terranes of western Ethiopia, northern Kenya, Somalia and the northern part of the Arabo-Nubian Shield is also suggested.

Adola Tectonothermal Event (1157±2 to 1030±40 Ma)

This tectonothermal event is inferred from ages of zircon xenocrysts (1125±2.5 Ma and 1156.8±1.9 Ma - Teklay et al. 1998; 1362±43 Ma - this study) obtained from the eastern part of the granite-gneiss terrane of the study area. The oldest metamorphic age (1030±40 Ma, Rb-

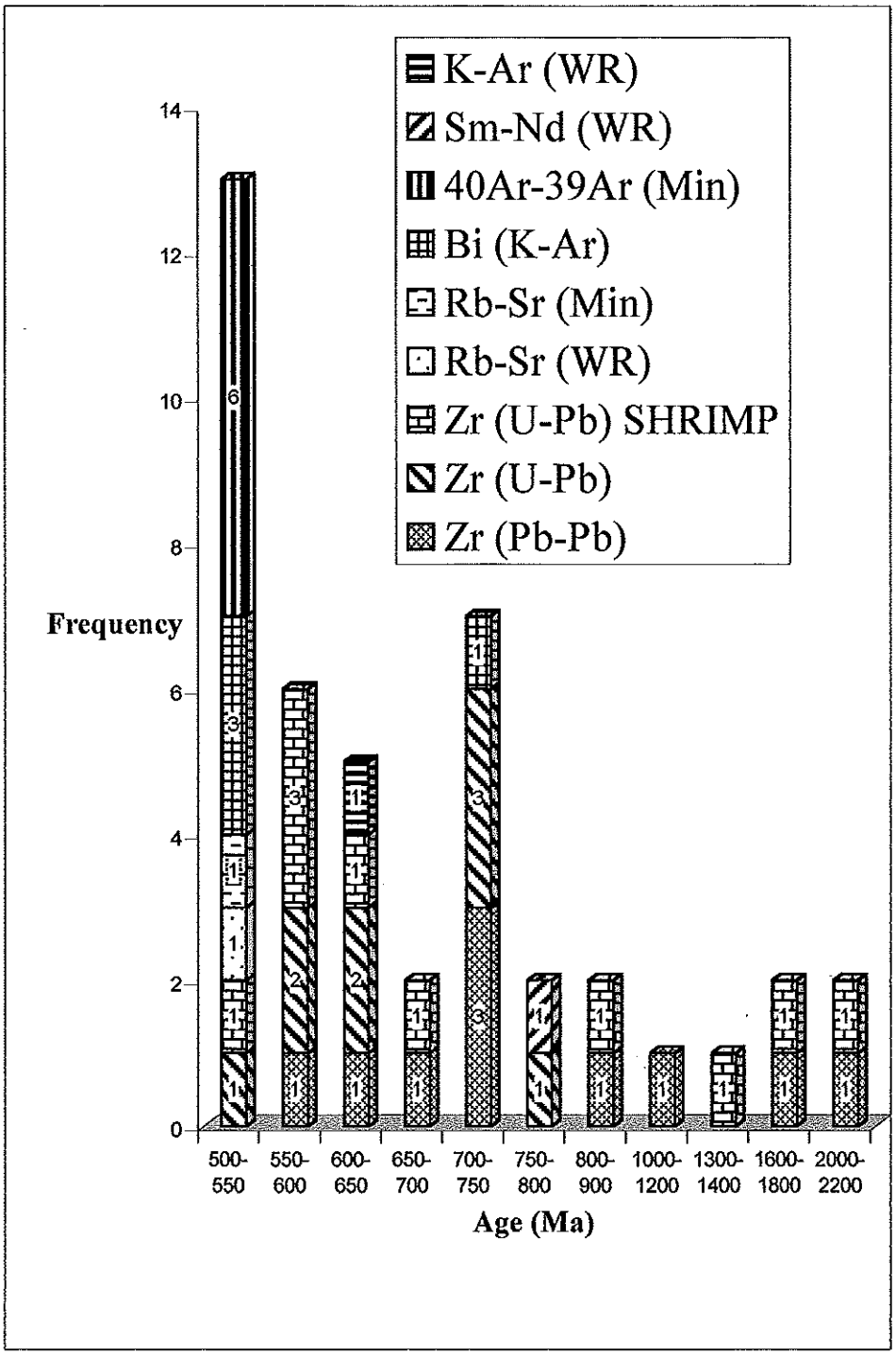

Figure 4: *Histogram of available geochronlogical data for the Precambrian of southern Ethiopia (this study and literature).*

Sr) in southern Ethiopia, obtained for the metasedimentary rocks of Adola (Chater, 1971), is used to constrain the upper limit of this tectonothermal event, the latter being correlated with the M0 metamorphic event of Worku (1996). In north-central Kenya, Key et al. (1989) inferred the existence of "cold migmatitic basement" of probable Kibaran age based on a 1200 Ma three-point isochron on leucosomes interpreted as the migmatisation age for the Mukogodo migmatite.

Bulbul-Awata Tectonothermal Event (~876±5 Ma)

Geochemical data for the granitoids of the study area (Yibas, 2000) suggest that the Bulbul diorite gneiss, which is dated as 876±5 Ma old, has a subduction-related geochemical affinity. This suggests that the first recognisable subduction-related tectonothermal event in the East African Orogen of southern Ethiopia began at about this time. The earliest Mozambican tectonothermal event in Kenya is the Samburian-Sabachian event at about 830 Ma (Key et al., 1989) - a period of amphibolite-granulite facies metamorphism and recumbent folding related to plate collision oblique to the north-south strike of the orogen, between the Archaean Tanzanian Craton in the west and an eastern Kibaran Craton (Key et al., 1989; Charsley, 1987).

Megado Tectonothermal Event (770-720 Ma)

A Sm-Nd isochron age of 789 ± 36 Ma for the Megado metavolcanics (Worku, 1996), a circa 778-760 Ma U-Pb zircon SHRIMP age (this study) and an U-Pb zircon age by Genzebu et al. (1994) for some granitoids imply the presence of a strong tectonothermal event during this period, possibly associated with subduction of the Megado oceanic basin (Yibas, 2000). These granitoids are geochemically classified into those emplaced either in attenuated continental crust or in a subduction-related setting associated with the closure of the Megado oceanic basin and obduction of the ophiolite (Yibas, 2000). The associated peak metamorphism was dated at 749±15 Ma for the El Der hornblende-biotite gneiss (K-Ar date - Rogers et al., 1965). In the western part of the study area, high metamorphic pressure (~ 9 kbar), under which granulites formed, indicates significant crustal thickening related to major collision–induced thrusting (Gichile, 1991, 1992). This period is recognised in western Ethiopia as a period of regional metamorphism (759±18 Ma Rb-Sr and 783±15 U-Pb, Ayalew et al., 1990) coincident with the age of many "ophiolites" in the Arabo-Nubian Shield (Mosley et al., 1993). Emplacement of allochthonous ophiolites and volcanosedimentary "packages", coupled with thrusting and imbrication of paragneiss groups in Kenya, took place at about 760 Ma (Rb-Sr emplacement age - Cahen et al., 1984). The period between 710 and 730 Ma was dominated by emplacement of charnockitic rocks in southern Ethiopia (e.g., Yabello charnockitic granite-gneiss, Sagan basic charnockite, and Konso granulite of 725±Ma, 716±5, 721±12 Ma age, respectively - Teklay et al., 1993, 1998). This event could be correlative with the widespread presence of charnockitic granites and granulite facies metamorphism from Sudan to Tanzania (Stern and Dawoud, 1991; Maboko et al., 1995) and farther south into Malawi (Kröner, 1993). Kröner argued that this age might be the age of the emplacement of the precursors of the granulitic rocks, and that the granulite facies metamorphism could be related to Pb-loss at 538+49/-35 Ma. This was the case at least for the Wami River granulites of Tanzania and the Konso granulites of southwestern Ethiopia (Kröner, 1993).

Moyale Tectonothermal Event (700-550 Ma)

The fourth tectonothermal event in southern Ethiopia, which could possibly have taken place between 700 and 550 Ma, is related to the closure of the Moyale oceanic basin (Yibas, 2000). A protracted period of subduction-related granitic magmatism followed (Moyale granodiorite emplaced at 666±5 Ma; Digati diorite gneiss at 570±7 Ma; Wadera granite-gneiss at 575±5 Ma; U-Pb SHRIMP ages, this study; the Gariboro collisional granitoids - 602-646 Ma, U-Pb, Worku, 1996; and the Meleka granodiorite at 610±9 Ma - U-Pb SHRIMP, this study). The Rb-Sr ages of 680±10 Ma (Gilboy, 1970) and 594-605 Ma (Worku, 1996) for the Gariboro and Burjiji granitoids could be associated with a collision-induced metamorphic event (Gilboy, 1970; Worku, 1996; Yibas, 2000). This is possibly correlative with the Baragoian-Barsaloian tectonothermal event (630-580 Ma), which resulted in amphibolite facies metamorphism in Kenya (Key et al., 1989).

Berguda Tectonothermal Event (550-500 Ma)

This period, which marks the end of the Pan African orogeny in this region, was manifested by emplacement of late- to post-tectonic granitoids throughout southern Ethiopia. However, evidence of granulite facies metamorphism during this period is seen in the presence of the charnockitic Berguda granitoid in the western part of the study area (Gichile, 1991, 1992; Yibas, 2000). Gichile (1992) recognised a metamorphic signature and intense deformation in the core of this layered granitoid and suggested that the Berguda granitoid is a tectonically uplifted block. Two U-Pb (zircon) ages were obtained for this pluton (Genzebu et al., 1994), one for the granulitic core and another for the so-called intermediate zone, at 538±2.8 Ma and 528±8.4 Ma, respectively. These ages are similar to the ages of other Pan-African granulites in other parts of the East African Orogen, where granulite facies metamorphism and associated deformation occurred between 553 and 521 Ma, which is the postulated time of initial Gondwana amalgamation (Jacobs et al., 1995). The presence of strongly deformed and metamorphosed granulitic granites and undeformed granitoids, having similar zircon ages, suggests the simultaneous emplacement of these granitoids into the different parts of the crust and juxtaposition of these granitoids by thrusting and transcurrent faulting and shearing, associated with uplifting and final cooling.

The youngest granite age thus far recorded in the Precambrian of southern Ethiopia is that of the 526 Ma Metoarbasebat granite (SHRIMP zircon dating, this study). The ^{40}Ar-^{39}Ar ages of biotite, muscovite and hornblende grains from selected granitoids range from 495±5 to 515±3 Ma and are, thus, included here under the age of the Berguda Tectonothermal Event.

The Berguda Tectonothermal Event also coincides with Rb-Sr whole rock isochron ages and a U-Pb date of circa 582 to 541 Ma, which are interpreted as bracketing the last metamorphism and deformation in western Ethiopia (Ayalew et al., 1990). In Kenya, this event correlates with an ~500-480 Ma event, which has been interpreted as the period of uplift, high level thrusting, emplacement of pegmatites and melts, and final cooling (Key et al., 1989; Mosley, 1993).

A 516±3 Ma ^{40}Ar-^{39}Ar age was obtained for muscovite grains from the Lega Dembi gold deposit (Table 3; see also Mechessa, 1996). This age is indistinguishable from all other ^{40}Ar-^{39}Ar ages obtained for the granitoids of southern Ethiopia, and is interpreted to be a resetting age due to the Berguda Tectonothermal Event (550-500 Ma). Yibas (2000) has shown, on the basis of integrated structural and geochronological data, that the Moyale Tectonothermal

Event (700-550 Ma) was mainly responsible for creating favourable structures in southern Ethiopia, which served as hydrothermal fluid conduits for the remobilization and concentration of gold mineralisation into its present location.

SUMMARY

1. The combined use of SHRIMP and laser probe $^{40}Ar/^{39}Ar$ dating, coupled with previously available data and field mapping, suggests that the granitoids of the Precambrian of southern Ethiopia can be classified into seven generations [Gt1 (>850 Ma), Gt2 (800-770 Ma), Gt3 (770-720 Ma), Gt4 (720-700 Ma), Gt5 (700-600 Ma), Gt6 (580-550 Ma), and Gt7 (550-500 Ma)]. With the exception of the Gt7 granitoids, all other granitoids show variable intensities of deformation (Yibas, 2000).

2. The period 550 to 500 Ma (Gt7) is marked by the emplacement of late- to post-tectonic and post-orogenic granitoids, such as the Metoarbasebat granite. It is associated with uplift and final cooling marking the end of the East African Orogen. This interpretation is supported by the ^{40}Ar-^{39}Ar ages obtained from all the granitoids dated in this study. Although the magmatic ages obtained from the SHRIMP zircon dating range from 526 Ma to 880 Ma, the ^{40}Ar-^{39}Ar ages for all these samples are younger that 550 Ma. This suggests that this period represents the latest tectonothermal event.

3. Five tectonothermal events of the East African Orogen are recognised in the Precambrian of southern Ethiopia. These are the Adola (1157±2 to1030 ± 40 Ma), Bulbul-Awata (~876 ± 5 Ma), Megado (800-750 Ma), Moyale (700-550 Ma) and Berguda (550-500 Ma) tectonothermal events.

4. The period between 710 and 730 Ma was dominated by the emplacement of charnockitic rocks (Yabello charnockitic granite-gneiss, Sagan basic charnockite, and Konso granulite) in southern Ethiopia. This event may correlate with the widespread presence of charnockitic granites and granulite facies metamorphism from Sudan to Tanzania (Maboko et al., 1995) and further south into Malawi, but this suggestion is not universally accepted (e.g., Kröner, 1993).

5. The presence of granulite facies metamorphism in southern Ethiopia at the end of the Pan-African orogeny is evidenced by the charnockitic Berguda Granitoid in the western part of the study area (~ 530 Ma). This age is similar to the ages of Pan-African granulites in other parts of the East African Orogen where granulite facies metamorphism and associated deformation occurred between 553 and 521 Ma - the postulated time of initial Gondwana amalgamation (Jacobs et al., 1995).

6. The integration of structural and geochronological data has shown that the Moyale Tectonothermal Event (700-550 Ma) must have been responsible for creating the most favourable structures in southern Ethiopia for gold mineralisation. These structures served as fluid conduits for the hydrothermal systems that remobilized and concentrated the gold mineralisation into its present location (Yibas, 2000). Therefore, the ^{40}Ar-^{39}Ar age of 516±3 Ma obtained on muscovite grains from a gold-bearing quartz vein from the Lega Demgbi gold deposit does not indicate the age of mineralisation, but rather the age of the reworking of the mineralisation due to the Berguda Tectonothermal Event (550-500 Ma).

ACKNOWLEDGEMENTS

This paper has resulted from the PhD project by B. Yibas, which benefited from generous financial support from Anglo American Prospecting Services, Johannesburg. The Geological Survey of Ethiopia is thanked for granting permission to conduct this study. Lyn Whitfield and Di Du Toit provided drafting support.

REFERENCES

Abraham, A., Hassen, N., Yemane, T., Genzebu, W., Seyid, G., Mehari, K., and Alemu, T., 1992. The geological evolution of the Proterozoic of southern Ethiopia. Abstract, 29th International Geological Congress 2, Kyoto, Japan, p. 13.

Alemu, T., 1997. *Petrology, geochemistry and geochronology of the granitoids of Axum area, northern Ethiopia.* M.Sc. thesis (unpubl.), Institute of Petrology, University of Vienna, Austria, 106 pp.

Ayalew, T. and Gichile, S., 1990. Preliminary U-Pb ages from southern Ethiopia. Extended Abstract, 15th Colloquium of African Geology, Nancy, 127-130.

Ayalew, T., Bell, K., Moore, J. M. and Parrish, R. R., 1990. U-Pb and Rb-Sr geochronology of the western Ethiopian Shield. Geol. Soc. Am. Bull., **102**, 1309-1316.

Barbarin, B., 1990. Granitoids: main petrogenetic classifications in relation to origin and tectonic setting. Geol. J., **25**, 227-238.

Bonavia, F. F. and Chorowicz, J., 1993. Neoproterozoic structures in the Mozambique Belt orogenic belt of southern Ethiopia. Precambrian Research **62**, 307-322.

Cahen, N. Snelling, N. J., Delhal, J., and Vail, J. R., 1984. *The Geochronology and Evolution of Africa,* Clarendon Press, Oxford, 512 pp.

Charsley, T. J., 1987. Geology of the Laisamis area. Geological Survey Kenya, Nairobi, 106pp.

Chater, A. M., 1971. *The geology of the Megado region of southern Ethiopia.* Ph.D. thesis (unpubl.), University of Leeds, UK, 343 pp.

Compston, W., Williams, I. S., Kirschvink, J. L., Zhang, Z. and Ma, G., 1992. Zircon U-Pb ages for the Early Cambrian time-scale. Journal of Geological Society of London **149**, 171-184.

Cumming, G.L. and Richards, J.R., 1975. Ore lead isotope ratios in a continuously changing Earth. Earth Planetary Science Letters **28**, 155-171.

Genzebu, W., Hassen, N., and Yemane, T., 1994. Geology of the Agere Mariam area. Memoir, Ethiopian Inst. Geol. Survey, Addis Ababa, **8**, 23 pp.

Gichile, S., 1991. *Structure, metamorphism and tectonic setting of a gneissic terrane, the Sagan-Aflata area, southern Ethiopia, 1991.* M.Sc. thesis (unpubl.), University of Ottawa, Canada, 224 pp.

Gichile, S., 1992. Granulites in the Precambrian basement of southern Ethiopia: geochemistry, P-T conditions of metamorphism and tectonic setting. Journal of African Earth Sciences **16**, 251-263.

Gilboy, C. F., 1970. *The geology of the Gariboro region of southern Ethiopia.* Ph.D. thesis (unpubl.), University of Leeds, UK, 346 pp.

Guo, A. and Dickin, A. P., 1996. The southern limit of Archaean crust and significance of rocks with Palaeoproterozoic model ages: Nd model age mapping in the Grenville province of western Quebec. Precambrian Research 77, 231-241.

Haider, A., 1989. *Geologie de la formation ferrifère Precambrienne et du complèxe granulitique de Buur (Sud de le Somalie). Implications sur l'evolution crustale du socle de Buur.* Ph. D. thesis (unpubl.), INPL, Nancy, France, 157pp.

Jacobs, J., Ahrendt, H., Kreuzer, H. and Weber, K., 1995. K-Ar, ^{40}Ar-^{39}Ar and apatite fission-track evidence for Neoproterozoic rejuvenation events in the Heimfrontfjella and Manifault Knausana (East Antarctica). Precambrian Research **75**, 251-262.

Jelenc, D. A., 1966. *Mineral Occurrences of Ethiopia.* Ministry of Mines, Addis Ababa, 720pp.

Kazmin, V., 1971. Precambrian of Ethiopia. Nature **230**, 176-177.

Kazmin, V., 1972. Geology of Ethiopia: explanatory note to the geological map of Ethiopia, 1:2 000 000. Ministry of Mines, Addis Ababa, 14pp.

Kazmin, V., 1975. The Precambrian of Ethiopia and some aspects of the Mozambique Belt. Bulletin of the Geophysical Observatory, Addis Ababa University **15**, 27-45.

Kazmin, V., 1976. Ophiolites in the Ethiopian Basement. Ethiopian Institute of Geological Surveys, Addis Ababa, Note No. **35**, 17pp.

Kazmin, V., Alemu Shiferaw and Tilahun Balcha, 1978. The Ethiopian basement: stratigraphy and possible manner of evolution. Geol. Rdsch., **67**, 531-546.

Key, R. M., Charsley, T. J., Hackman, B.D., Wilkinson, A.F. and Rundle, C.C., 1989. Superimposed upper Proterozoic collision-controlled orogenesis in the Mozambique Belt of Kenya. Precambrian Research **44**, 197-225.

Kozyrev, V., Girma Kebede, Safanov, Yu., Bekele W. Michael, Gurbanovich, G., Tewolde Medhin, T., Katvikov, Arijapor, A., 1985. Regional geological and exploration work for gold and other minerals in the Adola Goldfield, southern Ethiopia, Vol. II., Regional geological mapping and prospecting, Unpubl. Rep., Ethiopian Minerals Resources Corporation, Addis Ababa, 343pp.

Kröner, A., 1984. Late Precambrian plate tectonics and orogeny: a need to redefine the tern Pan-African. *In*: Klerkx, J. and Michot, J. (eds.), *African Geology*, Tervuren, Muse'e. R. l'Afrique Centrale, pp. 23-28.

Kröner, A., 1993. The Pan-African Belt of Northeastern and Eastern Africa, Madagascar, Southern India, Sri Lanka and East Antarctica. *In*: Thorweihe, U. and Schandelmeier, H. (eds.), *Terrane Amalgamation During Formation of Gondwana Supercontinent*, Geoscientific Research in Northeast Africa, Berlin, pp. 3-9.

Kröner, A., Linnebacher, P., Stern, R. J., Reischmann, T., Manton, W., and Hussien, I. M., 1991. Evolution of Pan-African Island arc assemblages in the southern Red Sea Hills, Sudan, and in southwestern Arabia, as exemplified by geochemistry and geochronology. *In*: Stern, R. J. and Van Schmus, W. R. (eds.), *Crustal Evolution in the Late Proterozoic*. Precambrian Research **53**, 99-118.

Kröner, A., Pallister, J. S., and Fleck, R. J., 1992. Age of initial oceanic magmatism in the late Proterozoic Arabian shield. Geology **20**, 803-806.

Kröner, A., and Sassi, F. P., 1996. Evolution of the northern Somali basement: new constraints from zircon ages. Journal of African Earth Sciences **22**, 1-15.

Lameyre, J. and Bonin, B., 1993. Granites in the main plutonic series. *In*: Didier, J. and Barbarin, B. (eds.), *Enclaves and Granite Petrology*. Developments in Petrology **13**, Chapman & Hall, London, pp.3-17.

Lebling, C., 1940. Forschungen im Boran-Land (Südabessinien). N. Jahrb. Min. Geol., **84**, 205-232.

Lenoir, J. L. and Haider, A., 1990. Contribution to the knowledge of the petrogenesis and geochronology of the basement complex of southern Somalia (Buur region). Abstract, 15th Colloquium of African Geology, CIEFEG Occasional Publications. Nancy, p. 269.

Lenoir, J. L., Kuster, D., Liegeois, J. P., Utke, A., Haider, A. Matheis, G. 1993. Geodynamic significance of contrasting Pan-African granitoid types in Somalia. *In*: Thorweihe, U. and Schandelmeier, H. (eds.), *Proceedings of the International Conference on Geoscientific Research in Northeast Africa*, Berlin, pp. 145-150.

Maboko , M .A. M., Boelriijk, N. A. I. M., Priem, H. N. A., and Verdurmen, E. A. T . 1995. Zircon U-Pb and biotite Rb-Sr dating of the Wami River granulites, eastern granulites, Tanzania: evidence for approximately 715 Ma old granulite-facies metamorphism and final Pan-African cooling approximately 475 Ma ago. Precambrian Research **30**, 361-378.

Mechessa, A., 1996. *Geochemistry, geochronology, and genesis of the Lega Dembi Gold Deposit in the Adola Goldfield of southern Ethiopia.* Ph.D. thesis (unpubl.), University of Vienna, Austria,167 pp.

Mohr, P.A., 1963. *The Geology of Ethiopia.* University College of Addis Ababa Press, Addis Ababa, Ethiopia, 268 pp.

Mosley, P. N., 1993. Geological evolution of the late Proterozoic "Mozambique Belt" of Kenya. Tectonophysics **221**, 223-250.

Paces, J. B. and Miller, J. D. 1989. Precise U-Pb ages of the Duluth Complex and related mafic intrusions, Northeastern Minnesota: geochronological insights to physical, petrogenetic, paleomagnetic and tectonomagmatic processes associated with the 1.1 Ga mid-continent rift system. Journal of Geophysical Research **98B**, 13997-14013.

Rogers, A., Miller, J. M. and Mohr, P. A., 1965. Age determinations of some Ethiopian basement rocks. Nature **206**, 1021-1026.

Stern, R. J. 1993. Tectonic evolution of the Late Proterozoic East African Orogen: constraints from crustal evolution of the Arabo-Nubian Shield and the Mozambique Belt. *In*: Thorweihe, U. and Schandelmeier, H. (eds.), *Proceedings of the International Conference on Geoscientific Research in Northeast Africa,* Berlin , pp. 73-74.

Stern R. J. and Dawoud, A. S., 1991. Late Precambrian (740 Ma) charnockite, enderbite, and granite from Jabel Moya, Sudan: a link between the Mozambique Belt and the Arabo-Nubian Shield? Journal of Geology **99**, 648-659.

Stacey, J. S. and Agar, R. A., 1985. U-Pb isotopic evidence for the accretion of a continental micro-plate in the Zalm region of the Saudi Arabian Shield. Journal of the Geological Society of London **142**, 1189-1203.

Stoesser, D. B. and Stacey, J. S. 1988. Evolution, U-Pb geochronology and isotope geology of the Pan-African Nabitah orogenic Belt of the Saudi Arabian Shield. *In*: El Galaby, S. and Greilling, R. O. (eds.), *The Pan-African Belt of Northeast Africa and Adjacent Areas*, Vieweg, Braunschweig/Wiesbaden, pp. 227-288.

Tadesse, T., Suzuki, K., Hoshino, M., 1997. Chemical Th-U-total Pb isochron age of zircon from the Mereb granite in northern Ethiopia. Journal of Earth Planet. Science, Nagoya University, Japan **44**, 21-27.

Tadesse, T., Hoshino, M., Suzuki, K. and Iizumi, S., 2000. Sm-Nd, Rb-Sr and Th-U-Pb zircon ages of syn- and post-tectonic granitoids from the Axum area of northern Ethiopia. Journal of African Earth Sciences **30**, 313-327.

Teklay, M., Kröner, A., and Oberhansli, R., 1993. Reconnaissance Pb-Pb zircon ages from Precambrian rocks in eastern and southern Ethiopia and an attempt to define crustal provinces. *In*: Thorweihe, U and Schandlmeier, H. (eds.), *Geoscientific Research in Northeast Africa,* Balkema, Rotterdam, 133-138.

Teklay, M., Kröner, A., Mezger, K., and R. Oberhänsli, R., 1998. Geochemistry, Pb-Pb single zircon ages and Nd-Sr isotope composition of Precambrian rocks from southern and eastern Ethiopia: implications for crustal evolution in East Africa. Journal of African Earth Sciences **26**, 207-227.

Tera, F. and Wasserburg, G. J., 1972. U-Th-Pb systematics in three Apollo 14 basalts and the problem of initial Pb in lunar rocks. Earth Planet. Science Letters **14**, 281-304.

Turner, G., 1971. ^{40}Ar-^{39}Ar dating: the optimisation of irradiation parameters. Earth Planetary Science Letters **10**, 227-234.

Vail, J. R., 1976. Outline of the geochronology and tectonic units of the basement complex of Northeast Africa. Phil. Trans. R. Soc. London **A350**, 127-141.

Vail, J. R., 1985. Pan-African (late Precambrian) tectonic terrains and the reconstruction of the Arabian-Nubian Shield. Geology **13**, 839-842.

Vearncombe, J. R., 1983. A dismembered ophiolite from the Mozambique Belt, West Pokot, Kenya. Journal of African Earth Sciences **1**, 133-143.

Williams, I. S. and Claesson, S., 1987. Isotopic evidence for the Precambrian provenance and Caledonian metamorphism of high-grade paragneisses from the Seve Nappes, Scandinavian Caledonides. II. Ion microprobe zircon U-Th-Pb. Contribution to Mineralogy Petrology **97**, 205-217.

Windley, B. F., Whitehouse, M. J., Mahfood, A. O., and Ba-Bitat, M. A. O., 1996. Early Precambrian gneiss terranes and Pan-African island arcs in Yemen: crustal accretion of the eastern Arabian Shield. Geology **24**, 131-134.

Woldehaimanot, B., 1995. *Structural Geology and Geochemistry of the Neoproterozoic Adobha and Adola Belts (Eritrea and Ethiopia)*. Giess. Geol. Schriften, **54,** 218 pp.

Worku, H., 1996. *Geodynamic development of the Adola Belt (southern Ethiopia) in the Neoproterozoic and its control on gold mineralisation.* Ph.D. thesis (unpubl.), Berlin Technical University, 156 pp.

Worku, H. and Schandelmeier, H., 1996. Tectonic evolution of the Neoproterozoic Adola Belt of southern Ethiopia: evidence for Wilson Cycle process and implications for oblique plate collision. Precambrian Research 77, 179-210.

Yibas, B., 2000. *The Precambrian geology, tectonic evolution, and controls of gold mineralisations in southern Ethiopia.* Ph.D. thesis (unpubl.), University of the Witwatersrand, Johannesburg, 448 pp.

Yibas, B., Reimold, W. U. and Anhaeusser, C. R. 2000. The geology of the Precambrian of southern Ethiopia: I - The tectonostratigraphic record. Inform. Circ. Econ. Geol. Res. Inst., Univ. Witwatersrand, Johannesburg, **344**, 20 pp. (submitted to Journal of African Earth Sciences).

oOo